

1 **Identification of new leaf intrinsic yield genes using cross-species network analysis in plants**

2 Pasquale Luca Curci^{1,2,3}, Jie Zhang^{1,2+}, Niklas Mähler⁴⁺, Carolin Seyfferth^{1,2,4}, Chanaka
3 Mannapperuma⁴, Tim Diels^{1,2}, Tom Van Hautegeem^{1,2}, David Jonsen⁶, Nathaniel Street⁴, Torgeir
4 R. Hvidsten^{4,7}, Magnus Hertzberg⁶, Ove Nilsson⁵, Dirk Inze^{1,2}, Hilde Nelissen^{1,2}, Klaas
5 Vandepoele^{1,2,8*}

6 (1) Department of Plant Biotechnology and Bioinformatics, Ghent University, Technologiepark
7 71, 9052 Ghent, Belgium

8 (2) VIB Center for Plant Systems Biology, Technologiepark 71, 9052 Ghent, Belgium

9 (3) Institute of Biosciences and Bioresources, National Research Council (CNR), Via Amendola
10 165/A, 70126 Bari, Italy

11 (4) Umea Plant Science Centre (UPSC), Department of Plant Physiology, Umeå University,
12 90187 Umeå, Sweden.

13 (5) Umea Plant Science Centre (UPSC), Department of Forest Genetics and Plant Physiology,
14 Swedish University of Agricultural Sciences, 90183 Umeå, Sweden.

15 (6) SweTree Technologies AB, Skogsmarksgränd 7, SE-907 36 Umeå, Sweden

16 (7) Faculty of Chemistry, Biotechnology and Food Science, Norwegian University of Life
17 Sciences, 1432 Ås, Norway

18 (8) Bioinformatics Institute Ghent, Ghent University, Technologiepark 71, 9052 Ghent, Belgium

19 + both authors contributed equally

20 * corresponding authors: Klaas.Vandepoele@psb.vib-ugent.be

21 Short title: Identification of new intrinsic yield genes in plants

22 The author(s) responsible for distribution of materials integral to the findings presented in this
23 article in accordance with the policy described in the Instructions for Authors
24 (www.plantcell.org) is: Klaas Vandepoele (Klaas.Vandepoele@psb.vib-ugent.be).

25 **Abstract**

26 Plant leaves differ in their size, form and structure, and the processes of cell division and cell
27 expansion contribute to this diversity. Leaf transcriptional networks covering cell division and
28 cell expansion in *Arabidopsis thaliana*, maize (*Zea mays*) and aspen (*Populus tremula*) were
29 compared to identify candidate genes that are conserved in plant growth and ultimately have the
30 potential to increase biomass (intrinsic yield, IY). Our approach revealed that genes showing
31 strongly conserved co-expression were mainly involved in fundamental leaf developmental
32 processes such as photosynthesis, translation, and cell proliferation. Next, known intrinsic yield
33 genes (IYGs) together with cross-species conserved networks were used to predict novel
34 potential Arabidopsis leaf IYGs. Using an in-depth literature screening, 34 out of 100 top
35 predicted IYGs were confirmed to affect leaf phenotype if mutated or overexpressed and thus
36 represent novel potential IYGs. Globally, these new IYGs were involved in processes mostly
37 covering cell cycle, plant defense responses, gibberellin, auxin and brassinosteroid signaling.
38 Application of loss-of-function lines and phenotypic characterization confirmed two newly
39 predicted IYGs to be involved in leaf growth (*NPF6.4* and *LATE MERISTEM IDENTITY2*). In
40 conclusion, the presented network approach offers an integrative cross-species strategy to
41 identify new yield genes and to accelerate plant breeding.

42

43

44

45

46

47

48

49

50 **Introduction**

51 New plant organs are formed and then grow continuously throughout development. Upon
52 adverse conditions, growth adjustments are among the first plant responses, rendering growth
53 regulation an important yield component (Gray and Brady, 2016; Nowicka, 2019). The growth of
54 plants involves complex mechanisms controlling processes from the cellular to the whole-
55 organism level. Cell division and cell expansion are the two major processes regulating leaf
56 growth and previous research has shown that largely similar cellular and molecular pathways
57 govern these fundamental processes in dicots and monocots (Anastasiou et al., 2007; Nelissen et
58 al., 2016). Numerous genes have been identified that when mutated or ectopically expressed
59 increase organ size, such as leaf size, in plants. These so-called ‘intrinsic yield genes’ (IYGs) are
60 part of functional modules of genes/proteins that govern sub-processes that constitute organ
61 growth. Many of these genes are functionally conserved across plant species and some of these
62 genes promote, when mutated or ectopically expressed, organ growth in both dicots and
63 monocots. Notable examples are genes encoding CYP78A, ARGOS, rate limiting GA
64 biosynthesis enzymes, BRI1, ANGUSTIFOLIA3 and GROWTH-REGULATING FACTORS
65 (Powell and Lenhard, 2012; Vercruyse et al., 2020).

66 However, the complex and highly dynamic nature of the regulatory networks controlling such
67 complex traits makes the identification of new growth regulatory genes challenging (Baxter,
68 2020). Moreover, duplication events across the plant kingdom have caused a general
69 enlargement of gene families and, with it, plant- and tissue-specific functional specialization
70 (Jones and Vandepoele, 2020). Gene orthology information is essential to transfer functional
71 annotations from model plants with high quality annotations (e.g. *Arabidopsis thaliana*) to other
72 species. Functional annotations derived from experimental evidence can be used to identify
73 relevant orthologs and drive gene function discovery in crops (Lee et al., 2015, 2019). This
74 approach is not straightforward, mainly for two reasons: first, the orthology approach normally
75 leads to the identification of complex (one-to-one, one-to-many and many-to-many) orthology
76 relationships (Movahedi et al., 2011; van Bel et al., 2012); second, for genes with multiple
77 orthologs, it has been observed that the closest ortholog in terms of protein sequence similarity is
78 often not the closest ortholog in terms of regulation, indicating that identifying functionally
79 conserved orthologs is challenging (Patel et al., 2012; Netotea et al., 2014).

80 Biological networks offer the means to study the complex organization of gene interactions.
81 Densely connected network clusters form gene modules, defined as groups of linked genes with
82 similar expression profiles (i.e. co-expressed genes), which also tend to be co-regulated and
83 functionally related (Heyndrickx and Vandepoele, 2012; Klie et al., 2012). Although transferring
84 network links from better annotated species to crops is the most intuitive approach and has
85 proven to be helpful (Ficklin and Feltus, 2011; Obertello et al., 2015), it has been shown that
86 only ~20-40% of the co-expression links are conserved in pairwise comparison of *Arabidopsis*
87 *thaliana* (*Arabidopsis*), *Populus*, and *Oryza sativa* (Netotea et al., 2014). On the other hand, it
88 has been shown that using gene modules that are conserved across species can increase the
89 amount of biological knowledge transferred from one species to another (Mutwil et al., 2011;
90 Heyndrickx and Vandepoele, 2012; Cheng et al., 2021). Such conserved gene modules mirror
91 biological processes conserved across species, meaning that the orthologous genes present in
92 these modules are involved in the same process and potentially perform the same function
93 (Ruprecht et al., 2011). Significantly conserved cross-species modules (with many shared
94 orthologs) can be used to transfer gene function annotations and analyze expression conservation
95 for paralogs involved in complex many-to-many orthology relationships. A guilt-by-association
96 approach can also then be used to infer functions of unknown genes from the functions of co-
97 expressed annotated genes (Wolfe et al., 2005; Lee et al., 2010; De Smet and Marchal, 2010;
98 Klie et al., 2012; Rhee and Mutwil, 2014).

99 Here, we focused on high-resolution leaf transcriptomes covering cell proliferation and
100 expansion in three plant species: two dicotyledonous plants, the annual plant *Arabidopsis* and the
101 perennial plant *Populus tremula* (aspen), and one monocotyledonous plant, *Zea mays* (maize).
102 We constructed aggregated co-expression networks for each species, performed cross-species
103 comparison of these leaf development transcriptional networks and used conserved gene
104 neighborhoods to predict and validate new IYGs in *Arabidopsis* with the potential to increase
105 organ growth.

106

107

108 **Results**

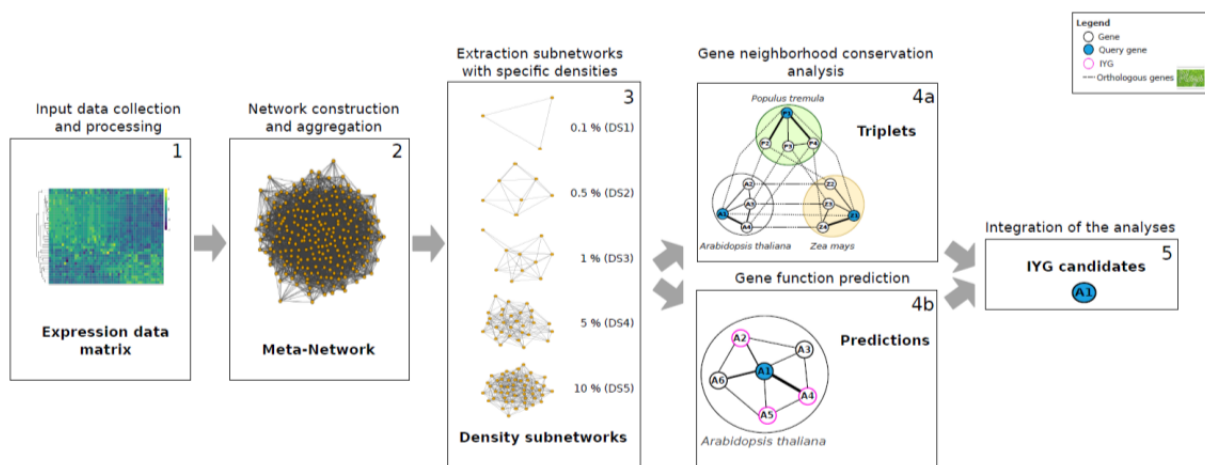
109 **Network construction and gene neighborhood conservation analysis**

110 To perform network construction based on gene expression information, expression compendia
111 were built for Arabidopsis, maize and aspen that contained a minimum of 24 leaf samples (Fig.
112 1, step 1; Table S1; Supplemental Methods). These expression compendia all include
113 developmental stages with active cell proliferation and cell expansion. The Arabidopsis
114 expression compendium was composed of three main developmental phases: cell proliferation,
115 cell expansion and the transition between these two phases. For maize, the developmental
116 expression compendium included a newly-generated high-resolution dataset and covers cell
117 proliferation, cell expansion and mature phases of development (Supplemental Methods). For
118 aspen, samples covered the developmental stages ranging from the very youngest leaf primordia
119 to fully expanded and mature leaves. In total, expression data covered 20,313 genes for
120 Arabidopsis, 29,383 genes for maize, and 35,309 genes for aspen (Dataset 1).

121 The network construction was performed for each species with Seidr, a toolkit to perform
122 multiple gene network inferences and combine their results into a unified meta-network
123 (Schiffthaler et al., 2018). For each network inference algorithm included, a fully connected
124 weighted gene network was constructed. These were in turn aggregated into a weighted meta-
125 network (Fig. 1, step 2). When applying a weight threshold, the network density was defined as
126 the ratio between the number of links with a weight higher than this threshold and the number of
127 links in the weighted network. To dissect the network structure, several thresholds were used to
128 subset the meta-networks into more stringent density subnetworks (DSs). For each species meta-
129 network, five DSs were obtained ranging from DS1 (top 0.1% links) with an average of 358,455
130 links, to DS5 (top 10% links) with an average of 35,845,512 links (Fig. 1, step 3), with higher
131 densities corresponding to a higher number of neighbors for each gene in the network (Fig. S1).

132 To identify genes showing conserved co-expression in different species, a gene neighborhood
133 conservation analysis was performed using each DS and the information on the orthology
134 relationships between Arabidopsis, maize and aspen genes (Fig. 1, step 4a). The network
135 neighborhood of a gene is represented by all genes connected to it, at a given threshold. This
136 concept was used to identify conserved “triplets” (Dataset 2), each containing three orthologous
137 genes across Arabidopsis, maize and aspen with statistically significant overlaps of their gene

138 network neighborhoods. In an example triplet (Fig. 1, step 4a), a specific Arabidopsis gene *AI*,
139 will have an ortholog *ZI* in maize and another ortholog *PI* in aspen and these three genes will
140 have a significant overlap of their gene network neighborhoods. Due to the complex orthology
141 relationships that exist in plants, each gene can belong to one or multiple triplets as it can have
142 one or more orthologs. For example, an Arabidopsis gene with only one ortholog in maize and
143 aspen, assuming they have significant overlap of their gene network neighborhoods, will belong
144 to one triplet. In contrast, another Arabidopsis gene with two orthologs in maize and three in
145 aspen, assuming they also all have significant overlaps of their gene network neighborhoods, will
146 belong to six triplets. We refer to the set of unique genes that are part of triplets as “triplet
147 genes”. Next, the conserved gene neighborhoods were used to dissect the complex network
148 structures of these plants and to functionally harness the orthology relationships. The cross-
149 species networks are available in an interactive web application ([https://beta-](https://beta-complex.plantgenie.org)
150 [complex.plantgenie.org](https://beta-complex.plantgenie.org)).



151

152 **Figure 1. Outline of the cross-species network approach to identify new intrinsic yield gene**
153 **candidates.** For Arabidopsis, maize and aspen, the expression data (step 1) is used as input to
154 construct a fully connected meta-network per species (step 2). Subsequently each meta-network
155 is split into five density subnetworks (DSs) by applying specific density cutoffs (step 3). These
156 DSs are the input for two different analyses: they are used first as input to compute cross-species
157 gene neighborhood conservation (step 4a). Secondly, they are used to predict new functions via
158 guilt-by-association (step 4b). This leads to gene function annotations of query genes (blue
159 circles) based on prior knowledge on IYGs (purple circles). Edge thickness defines in which
160 subnetwork the interaction is conserved (line thickness represents the DS and ranges from 1, the
161 most stringent DS represented by the thickest line, to 5, the least stringent DS represented by the
162 thinnest line). Finally, the results of these two analyses (steps 4a and 4b) are integrated to obtain
163 a list of IYG candidates (step 5).

164

165 **Delineation of conserved intrinsic yield genes contributing to leaf growth**

166 Since the output of cell proliferation and expansion are strongly contributing to leaf size, we
167 hypothesized that the generated triplets were an excellent source to extract orthologs potentially
168 affecting plant leaf growth (intrinsic yield genes (IYGs)). An IYG is defined as a gene that when
169 inactivated or ectopically expressed increases organ size, here leaf size, by stimulating cell
170 proliferation (and thus higher cell number, as in the case of GRF (GROWTH-REGULATING
171 FACTOR) and GIF (GRF-INTERACTING FACTOR) proteins (Lee et al., 2009)) and/or cell
172 expansion (as in the case of *ZHD5* (*ZINC-FINGER HOMEODOMAIN 5*) (Hong et al., 2011)).
173 We generated a list of known IYGs from all three plant species (“primary-IYGs”) composed of
174 71 primary-IYGs from Arabidopsis, 71 from aspen and eight from maize. This list of genes was
175 obtained by collecting scientific literature and by large-scale phenotypic screenings of mutant
176 and over-expression of Arabidopsis, maize, and aspen (Table S2).

177 We then used the triplets to transfer IYGs from maize and aspen to Arabidopsis (“translated-
178 IYGs”). Briefly, primary-IYGs from maize and aspen, also identified as triplet genes, were used
179 to extract Arabidopsis orthologs with conserved co-expression. The primary-IYGs and
180 translated-IYGs were finally merged and filtered for high expression variation in the Arabidopsis
181 expression compendium to retain only those active during either cell proliferation or cell
182 expansion. The resulting set, named “expression-supported IYGs” (Table S2, Fig. S2), was
183 composed of 82 IYGs, including 24 Arabidopsis primary-IYGs and 58 translated-IYGs (*GRF2*
184 and *GA20OX1* (*GIBBERELLIN 20-OXIDASE 1*) were shared between primary-IYG and
185 translated-IYG sets). According to their expression profile in Arabidopsis, 35 expression-
186 supported IYGs showed maximal expression during cell proliferation, including several
187 proliferation marker genes like GROWTH-REGULATING FACTORS (e.g. *GRF1*, *GRF2*,
188 *GRF3*), AINTEGUMENTA (*ANT* (Mizukami and Fischer, 2000) and *KLUH* (Anastasiou et al.,
189 2007)), and 47 expression-supported IYGs had increased expression during cell expansion, such
190 as *GA20ox1* (Barboza et al., 2013) and *BR ENHANCED EXPRESSION 2* (*BEE2* (Friedrichsen et
191 al., 2002)).

192 The 82 expression-supported IYGs (from here on simply referred to as “IYGs”) represented our
193 “guide” set of yield-related genes, obtained by the integration of prior knowledge on plant

194 growth and the cross-species gene neighborhood conservation approach, to identify new
195 candidate IYGs.

196

197 **Functional analysis of cross-species conserved networks underlying leaf cell proliferation** 198 **and expansion**

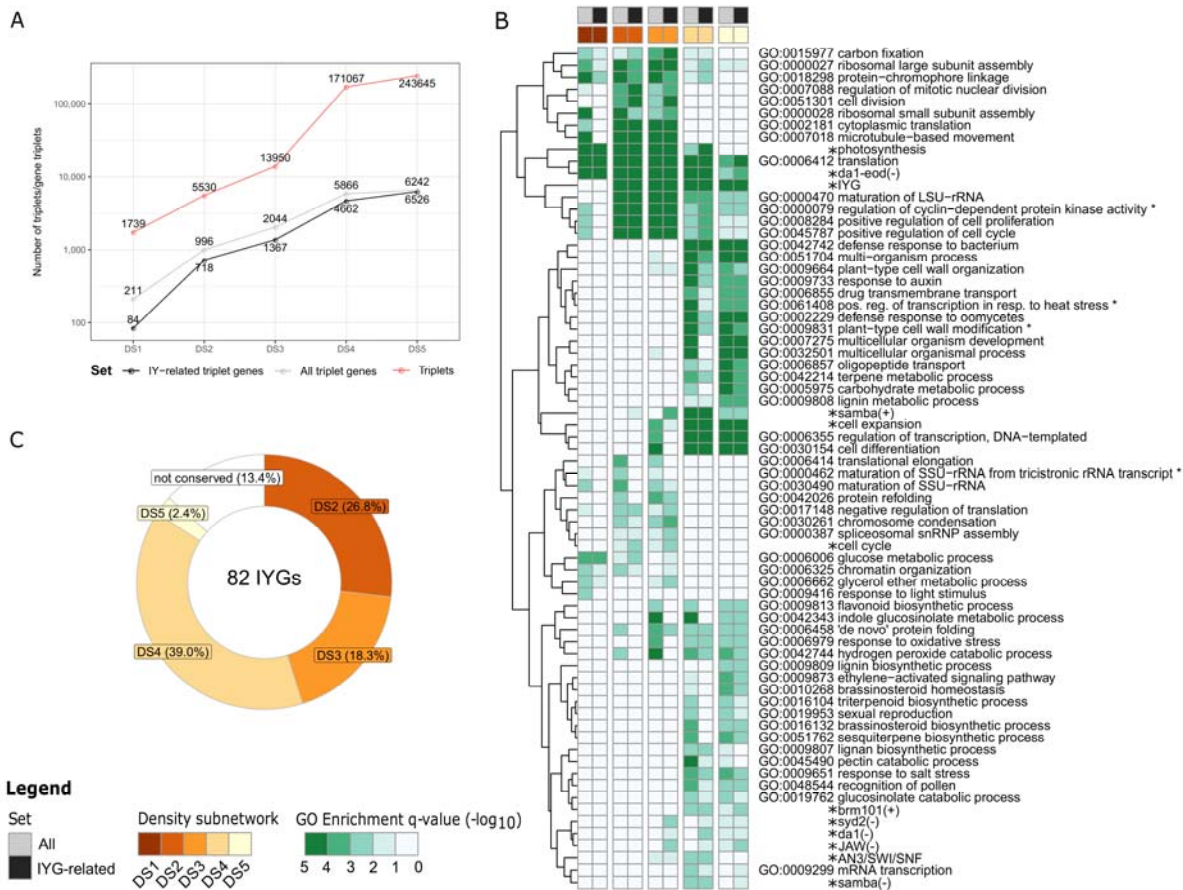
199 To explore cross-species conserved genes that function during cell proliferation and expansion,
200 we performed a Gene Ontology (GO (Ashburner et al., 2000)) functional enrichment analysis of
201 the Arabidopsis triplet genes from each DS across two sets: (1) all triplet genes (All) and (2) the
202 subset of triplet genes including the 82 IYGs and their co-expressed triplet genes (IYG-related
203 triplet genes) (Fig. 2). The total number of triplets ranged from 1,739 (DS1) to 243,645 (DS5)
204 (Fig. 2A; Dataset 2). To assess the significance of these numbers, a permutation approach was
205 employed where the orthology relationships were randomized 500 times and the number of
206 triplets obtained from each permutation was recorded. The number of triplets observed were
207 highly significant with not a single permutation for any DS exceeding the number of triplets
208 observed in the non-permuted data (p -value <0.002). The number of unique Arabidopsis triplet
209 genes ranged from 211 (DS1) to 6,526 (DS5) indicating that less sparse networks tend to have
210 more genes and more conserved gene neighborhoods (Fig. 2A). Interestingly, IYGs and their
211 network neighbors on average made up 71% of the triplet genes across the five DSs, suggesting
212 that plant growth-related gene networks are well conserved during leaf development across plant
213 species. For simplicity, from here on we will refer to triplet genes at a specific DS as, for
214 example at DS1, as “genes conserved at DS1”. The functional enrichment (Fig. 2B) showed that
215 triplet genes from the most stringent subnetwork (DS1) were enriched for fundamental biological
216 processes during leaf development, including photosynthesis (e.g. glucose metabolic process,
217 response to light and carbon fixation), translation (e.g. large and small ribosomal subunits) and
218 cell proliferation (e.g. positive regulation of cell cycle, chromatin organization, microtubule-
219 based movement). Processes such as cell division and cell cycle regulation were significantly
220 enriched for genes conserved at DS2 and DS3, including genes coding for cyclins (type A, B, D
221 and P), cyclin dependent kinases (*CDK*) and their subunits (*CKS*), and other genes involved in
222 the spindle formation (i.e. *MICROTUBULE-ASSOCIATED PROTEINS (MAP)65-4 and -5*). Cell
223 expansion-related processes were identified among genes conserved at DS3 and included genes

224 coding for expansins (EXP) and xyloglucan endotransglucosylases/hydrolases (XTH). Genes
225 conserved at the two least stringent subnetworks (DS4 and DS5) were enriched for GO terms
226 related to cell wall organization (e.g. lignan biosynthesis, pectin degradation, lignin metabolism),
227 defense response to biotic and abiotic stresses (e.g. defense response to oomycetes, response to
228 salt stress and heat stress), and transmembrane transport and hormone signaling (e.g. response to
229 auxin, ethylene and brassinosteroid). The category “regulation of transcription” was enriched for
230 genes conserved at DS3, DS4, and DS5. IYGs were significantly over-represented at DSs
231 starting from DS2, indicating that IYGs have highly conserved gene network neighborhoods.
232 Most of the IYGs (87%) were conserved in one or more DSs (mainly DS4) (Fig. 2C).

233 Among the IYGs conserved at DS2, 32% were transcription factors (TFs), including regulators
234 of cell cycle (e.g. *AINTEGUMENTA*) and cell elongation such as *BEE2* and its homolog *HBII*
235 (Fig. S3). These results suggest a conserved role of these TFs in leaf development across the
236 three plant species. Genes involved in hormone-mediated transcriptional regulation
237 (*INDOLEACETIC ACID-INDUCED PROTEIN (IAA)3*, *IAA14*, *IAA30*, and *AUXIN RESISTANT*
238 (*AUX1*) were also detected. Cell growth regulators, including the GRF family, were found
239 conserved and among them, *GRF2* was conserved at DS2. Literature information on
240 differentially expressed gene (DEG) sets from perturbation experiments was also included in the
241 functional enrichment analyses for several primary-IYGs. In particular, genes up- and down-
242 regulated in *SAMBA* loss-of-function mutants (Eloy et al., 2012) and *JAW (JAGGED AND*
243 *WAVY)* overexpression lines (Gonzalez et al., 2010) were significantly enriched in the IYG-
244 related set (Fig. 2B). Whereas *SAMBA* plays a key role in organ size control (seeds, leaves and
245 roots), transgenic overexpression lines of *JAW* showed enlarged leaves and an increased cell
246 number, indicative of prolonged cell proliferation (Gonzalez et al., 2010; Eloy et al., 2012). An
247 additional functional enrichment analysis was performed focusing on TF families to identify
248 their cross-species conservation level. In particular, genes conserved from DS2 to DS (Fig. S4)
249 were significantly enriched for the ETHYLENE RESPONSE FACTOR (ERF) family (q-value <
250 0.01), which has a recognized role in plant growth (Dubois et al., 2018). At DS3, among others,
251 MYB and WRKY TF families, known to be involved in developmental processes, appeared
252 strongly conserved. At the least stringent DSs (DS4 and DS5) we could observe other conserved
253 TF families like DOF (regulating the transcriptional machinery in plant cells), MIKC-MADS
254 (involved in floral development) and NAC (with functions in plant growth, development and

255 stress responses) (Lehti-Shiu et al., 2017). For TFs conserved at DS2, a significant enrichment
 256 was observed for the CONSTANS-like TF-family when considering IY-related triplet genes and
 257 included *BBX3*, *BBX4*, *BBX14* and *BBX16*. A number of BBX proteins have been linked with
 258 photomorphogenesis, neighborhood detection, and photoperiodic regulation of flowering
 259 (Vaishak et al., 2019).

260



261

262 **Figure 2. Triplets and their functional enrichments in cross-species conserved leaf**
 263 **networks.** (A) The number of triplet genes showing cross-species neighborhood conservation is
 264 plotted for all density subnetworks (DSs). (B) The functional over-representation of biological
 265 processes of interest is summarized for two sets: all triplet genes (All) and for IYGs and their
 266 network neighbor (IYG-related) triplet genes, subset of all triplet genes, in each DS. (C)
 267 Overview of IYGs with (and without) cross-species neighborhood conservation in different DSs.

268

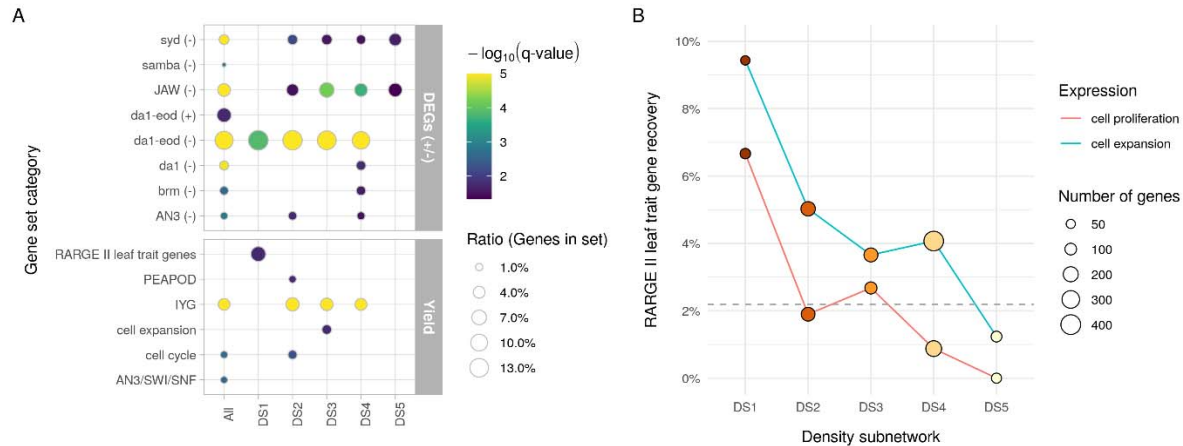
269 **Network-based prediction of novel IYGs**

270 Apart from analyzing the conservation level of known IYGs, we subsequently investigated if
271 new IYGs could be identified. To obtain high quality IYG predictions, a combined strategy was
272 adopted to leverage the known IYGs and the gene neighborhood conservation analysis through a
273 guilt-by-association (GBA) approach. The GBA principle states that genes with related function
274 tend to be protein interaction partners or share features such as expression patterns or close
275 network neighborhood (Oliver Stephen, 2000). First, gene function prediction through GBA was
276 performed, where guide IYGs were used for network exploration and gene function discovery
277 (Fig. 1, step 4b). New gene functions were assigned through functional enrichment in the
278 Arabidopsis networks, at different DSs. As a result, genes that were part of network
279 neighborhoods significantly enriched for known IYGs were classified as newly predicted IYGs,
280 and a GBA score was assigned to quantify the reliability of the predicted IYGs (Methods).
281 Secondly, the new predictions were filtered for those already identified as triplet genes (Fig. 1,
282 step 5). These filtered predictions, forming the predicted IYG set, were labelled with their
283 species names if they were already known as IYGs (primary or translated-IYG) or with “new” if
284 they were not (Table S4). This approach led to 2206 IYG predictions, of which 66 were known
285 IYGs. For the latter, 11 were uniquely from the Arabidopsis IYG primary set, 53 uniquely from
286 the aspen translated-IYGs, and the remaining two were shared among species. From DS1 to
287 DS5, the subsets of IYG predictions covered 175, 496, 421, 891 and 223 genes, respectively
288 (circle size in Fig. 3B) (Table S4). The expression profiles enabled identification of two major
289 clusters, with 1013 genes peaking at proliferation and 1193 at expansion phase (Table S4).

290 To evaluate the reliability of the predicted IYG set and its potential use for discovering genes
291 with a significant effect on plant growth, the public phenotype database RARGE II (Akiyama et
292 al., 2014), covering 17,808 genes and 35,594 lines, was screened obtaining a list of 391
293 Arabidopsis genes that, if mutated, caused a phenotype change in Arabidopsis leaf length, width
294 and/or size (RARGE II leaf trait genes, Table S5). Subsequently, functional enrichment was
295 applied to further investigate the predicted IYG set using these RARGE II leaf trait genes as well
296 as differentially expressed gene (DEG) sets from published yield-related perturbation
297 experiments (Fig. 3A). The RARGE II leaf trait gene set was significantly overrepresented only
298 in DS1, indicating that in stringent networks there is a higher chance of detecting genes causing a
299 visible phenotype if mutated (Fig. 3A). The gene set of downregulated genes in *dal-eod* double

300 mutants (Vanhaeren et al., 2017) was found enriched at DS1. These mutants showed
301 significantly increased cell size and cell number as compared to control due to processes taking
302 place before transition from cell proliferation to cell expansion delaying transition. The genes,
303 part of this set, were mostly coding for chloroplast proteins, involved in chloroplast development
304 (*LRGB*), light-harvesting (*LHCA2*), photosystems (*PSAD-2*, *OXYGEN EVOLVING COMPLEX*
305 *SUBUNIT 33 KDA (OEC33)*), and stomatal movement and conversion of carbon dioxide and
306 water (*CARBONIC ANHYDRASES (CA1, CA2, CA4)*). This suggests that genes active in
307 processes marking the onset of photosynthesis are well conserved across monocots and dicots. At
308 DS2 other sets of genes significantly overrepresented were those downregulated in plants
309 overexpressing *ANGUSTIFOLIA3 (AN3)*, and *JAW*, which carried larger leaves due to an
310 enhanced cell proliferation (Vercruyssen et al., 2014; Gonzalez et al., 2010). In common across
311 these two gene sets we found *AKT2*, which encodes for potassium inward channels that
312 contribute to the osmotically driven water uptake for expansion, and *DMR6*, a defense-associated
313 2OG-Fe(II) oxygenase. Among known IYGs conserved at any of the five DSs, we found
314 important genes acting at cell proliferation (e.g. *CYCD3*, *ANT*, *KLUH*, *GRF1*, *GRF3*, *GRF5*, and
315 *GIF2*) and others acting at cell expansion phase, such as *GA3OX1*, *GA20OX1*, and *GA20OX6*,
316 involved in the gibberellin biosynthetic pathway. Overall, cell proliferation genes were
317 statistically enriched at DS2 and expansion genes at DS3 (Fig. 3A). When investigating the gene
318 recovery for the RARGE II leaf trait genes (Fig. 3B), a clear trend was observed in phenotype
319 recovery ranging from DS1, with higher recovery (~3 and ~4.3 fold compared to what is
320 expected by chance for proliferation and expansion, respectively), to DS5, with almost no
321 recovery. This result indicates that the most stringent density subnetwork is a valuable source to
322 identify genes with a potential effect on leaf phenotype.

323



324

325 **Figure 3. Functional enrichment of the intrinsic yield gene predictions.** (A) Functional
 326 enrichment of the predictions split by density subnetwork. Gene sets in the upper panel were
 327 represented by upregulated (+) and downregulated (-) genes in overexpression lines (genes in
 328 upper-case) or mutant lines (genes in lower-case) collected from literature (Bezhani et al., 2007;
 329 Eloy et al., 2012; Vercruyssen et al., 2014; Vanhaeren et al., 2017). Gene sets in the lower panel
 330 were belonging to functional categories listed in Table S3. (B) Recovery of RARGE II leaf trait
 331 genes for each DS split in proliferation and expansion. The grey dashed line indicates the leaf-
 332 related phenotype gene recovery expected by chance (within the RARGE II dataset).

333

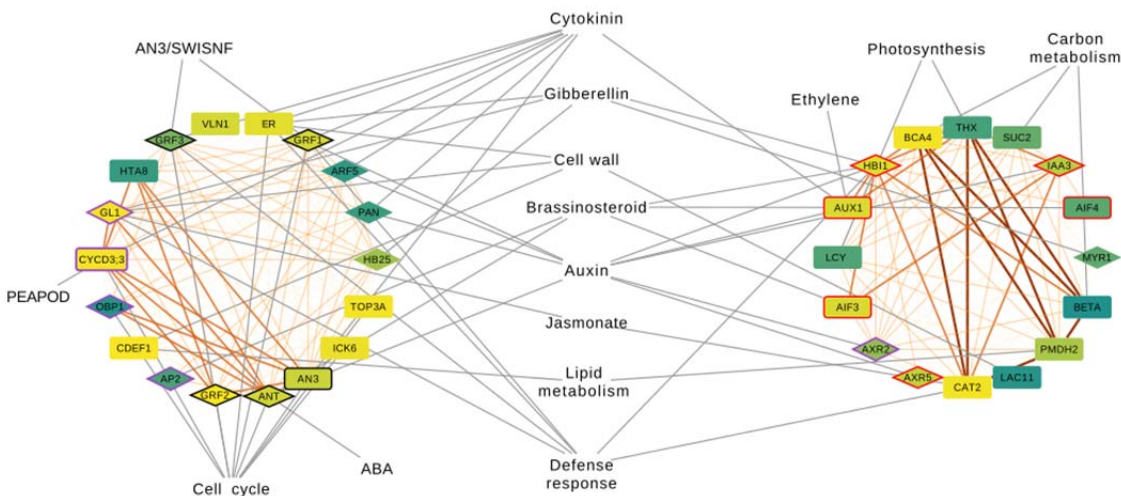
334 Validation of IYG predictions using literature and leaf phenotyping

335 To validate the assumption that the IYG predictions top ranked by GBA are more likely to show
 336 a phenotype, an in-depth literature analysis was performed to summarize the connection with
 337 yield pathways (Table S6) and to score known growth-related phenotypes for the top 100 IYG
 338 predictions (Table S7). For 61 of these 100 predicted genes, mutant lines and/or lines with
 339 ectopic expression were reported. For 34 out of the 61 genes (55.7%), obvious alterations to leaf
 340 size and shape as well as petiole length were reported when mutated or overexpressed, which
 341 included five Arabidopsis primary-IYGs, six translated-IYGs from aspen, and five paralogs to
 342 known IYGs (Fig. 4; Table S7). By screening the literature, these five IYG paralogs (*APETALA*
 343 *2* (*AP2*), *GLABRA 1* (*GL1*), *CYCD3;3*, *AUXIN RESISTANT 2* (*AXR2*), *OBP1*) were reported to
 344 show a leaf phenotype when mutated or overexpressed (Table S7).

345 Functional analysis of the 34 genes with described leaf phenotypes revealed their involvement in
 346 several biological processes and pathways such as cell cycle regulation, hormone response,
 347 photosynthesis, carbon utilization and cell wall modification (Fig. 4). Importantly, we could find
 348 conserved relationships between five specific genes active in the expansion phase: CATIONIC

349 AMINO ACID TRANSPORTER (*CAT2*), *THIOREDOXIN X* (*THX*), BETA CARBONIC
 350 ANHYDRASE (*BCA4*), *CA2*, and *PMDH2*. Among them, *CAT2* and *BCA4* were also high
 351 ranked by GBA score. For the proliferation cluster, we could observe strong relationships
 352 between *ANT*, *OBP1*, *GRF2*, *CYCD3;3*, *GLI*, *HTA8* (*HISTONE H2A 8*), and *AN3*. Among them,
 353 we identified TFs mainly involved in cell cycle process (*ANT*, *OBP1*, *GRF2*), cell wall (*GLI*),
 354 and hormone signaling pathways such as jasmonate (*GLI*), abscisic acid (*ANT*), and gibberellin
 355 (*GLI*). Twenty-seven of the 61 predictions with knock-down mutations and/or ectopic
 356 expression lines did not show a correlation with leaf growth, which may be partially due to the
 357 redundancy of large gene families or that the leaf phenotype was not explored in those studies.
 358 Additionally, three of these 23 genes have been reported to influence root or hypocotyl
 359 development, which may also contribute to overall plant growth and organ size.

360



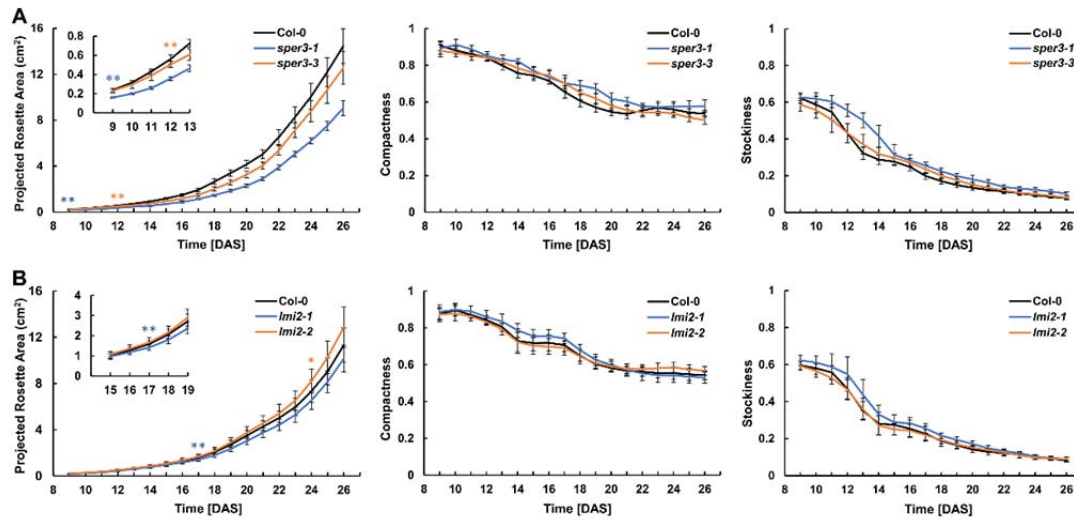
361

362 **Figure 4. Gene-function network of the 34 phenotype-related genes out of the top 100**
 363 **intrinsic yield gene predictions.** Predictions are clustered by expression profile (proliferation on
 364 the left and expansion on the right). Node label colours from yellow (strong) to dark green
 365 (weak) represent the reliability of the gene prediction (GBA score). Node border colours indicate
 366 known IYGs from Arabidopsis (black), known IYGs from aspen (red), and Arabidopsis known
 367 IYG paralogs (violet). Diamonds represent transcription factors. Links from dark orange thick
 368 (DS1) to light orange thin (DS5) represent the density subnetwork where the genes were found
 369 connected. Genes are linked to the yield pathway they are related with (centered if connecting to
 370 both proliferation and expansion related genes) by grey links. Anti-correlation links (connecting
 371 proliferation with expansion genes) were removed for clarity.

372

373 To further validate the role of these new IYGs in leaf development, we collected the mutants of
374 nine genes among the 27 predicted IYGs which have not been reported with a leaf phenotype
375 (Table S8). Molecular identification of these mutants was conducted and a detailed analysis of
376 leaf growth in controlled long-day soil-grown conditions was made (Fig. S5). By following the
377 projected rosette area (PRA), compactness and stockiness of each mutant line over time, this
378 phenotypic characterization revealed that the mutants of two IYG candidate genes showed
379 altered rosette growth. The mutant lines of a nitrate transporter gene *NPF6.4/NRT1.3*, *sper3-1*
380 and *sper3-3*, both displayed decreased PRA compared with the wild-type plants (Fig. 5A). The
381 *sper3-1* harbored a mutation at a conserved glutamate of *NRT1.3*, while the T-DNA line *sper3-3*
382 was a knockout allele (Tong et al., 2016). The reduction in size of *sper3-3* was smaller and
383 occurred later in development compared with *sper3-1*. Before bolting (26 DAS), *sper3-1* and
384 *sper3-3* were 37.3% and 13.2% smaller, respectively, compared with the wild-type (Table S8).
385 Besides *NPF6.4*, the mutants of *LATE MERISTEM IDENTITY2 (LMI2)* which has been reported
386 to be required for correct timing of the meristem identity transition (Pastore et al., 2011), also
387 showed altered rosette growth. In standard long-day conditions in soil, a significant reduction of
388 PRA was detected in *lmi2-1*, which displayed elevated *LMI2* expression in seedlings. By
389 contrast, the *lmi2-2* mutants in which the T-DNA insertion gave rise to a truncated non-
390 functional LMI2 protein, exhibited significantly increased PRA and were 13.5% larger than the
391 wild-type plants at 26 DAS (Fig. 5B and Table S8). Both *NPF6.4* and *LMI2* were highly ranked
392 by GBA (rank 18 and 20, respectively), which further implies that the predictions with a low
393 GBA score are more likely to show a leaf phenotype. Taken together, these experimentally
394 validated genes lend additional support to the potential of our predictions for plant growth.

395



396

397 **Figure 5. Mutants of IYG predicted genes *NPF6.4/NRT1.3* and *LMI2* showed altered**
398 **rosette growth.**

399 Dynamic growth analysis of projected rosette area, compactness and stockiness over time of
400 wild-type Col-0 and the mutants of *NPF6.4/NRT1.3* (A) and *LMI2* (B) in soil. The asterisks
401 represent the time points at which differences in the PRA become significant between the
402 mutants and wild-type, as determined by Student's *t* test (*, $P < 0.05$; **, $P < 0.01$).

403

404

405 Discussion

406 In this study, we aimed to identify candidate genes that would be robust targets for altering leaf
407 development using cross-species gene network analysis. To identify relevant context-specific
408 gene interactions, it is highly recommended to focus the gene network analysis on a specific
409 condition or context, rather than integrating multiple conditions (e.g. different stresses, growth
410 conditions, development stages) (Pavlidis and Gillis, 2012; Liseron-Monfils and Ware, 2015;
411 Serin et al., 2016). For this reason, expression datasets were generated and compiled capturing
412 two main features of leaf growth: cell proliferation and cell expansion. These two processes are
413 governed by similar cellular and molecular pathways across monocots and dicots (Nelissen et al.,
414 2016), which inspired the selection of transcriptional datasets from two dicots (*Arabidopsis* and
415 aspen) and one monocot (maize). The network construction was carried out integrating multiple
416 inference methods to leverage the power and complementarity of different network inference
417 algorithms (Marbach et al., 2012; Schiffthaler et al., 2018). To evaluate the strength of different
418 biological signals in our network, the gene interactions obtained after applying different network
419 density cutoffs (DS1-5) were studied. To identify functionally conserved genes across species,
420 we relied on two main approaches: the guilt-by-association principle, which is frequently used
421 for gene discovery, and network neighborhood conservation analysis, which detects significantly
422 overlapping network neighborhoods across species to identify reliable functional orthologs
423 (Movahedi et al., 2011; Netotea et al., 2014).

424 From the gene neighbourhood conservation analysis on five different density subnetworks, we
425 observed that, with an increased network density, the number of genes with conserved network
426 neighborhood also grew. This is expected and is probably due to a greater statistical power when
427 comparing larger neighborhoods (Netotea et al., 2014). Overall, as previously observed
428 (Vercruysse et al., 2020), the integration of different sequence-based orthology detection
429 methods was important because of their complementarity, highlighting complex orthology
430 relationships and evaluating the strength of the orthology support. Overall, 36% of the
431 *Arabidopsis* genes (7,320 out of 20,313 genes present in the network) had conserved
432 neighborhoods across *Arabidopsis*, aspen, and maize, in any of the five density subnetworks.
433 This result is similar to what has been found across *Arabidopsis*, poplar and rice, although a
434 different network construction pipeline was used there (Netotea et al., 2014).

435 From a plant breeding perspective, we were interested in focusing on cross-species conserved
436 targets with experimental evidence in more than one species. *GA20-oxidase1* represents a well-
437 known example of an IYG that is functionally conserved across monocots and dicots. This gene
438 was confirmed in our analyses to be conserved at the network neighbourhood level. *GA20-*
439 *oxidase1* is in fact a rate limiting enzyme for gibberellin growth hormone biosynthesis in
440 Arabidopsis, aspen, maize and rice (Gonzalez et al., 2010; Nelissen et al., 2012; Qin et al., 2013;
441 Eriksson et al., 2000). To validate the functional relevance of the predicted IYGs, we screened
442 the top 100 IYG predictions and observed that, among the 34 Arabidopsis predicted genes with a
443 known leaf phenotype in Arabidopsis, six were also already known to affect plant growth in
444 aspen (“translated-IYGs”). Plants, in fact, develop tissues and organs through the activity of both
445 primary and secondary meristems (vascular cambium) and there are overlapping regulatory
446 mechanisms between them (Baucher et al., 2007). The six translated-IYGs were *AUX1*,
447 *IAA3/SHY2*, *AXR5*, *AIF3*, *AIF4*, and *HBII* and their expression in Arabidopsis was peaking at the
448 cell expansion phase. The first three genes are auxin-related genes. Auxin is important for
449 regulating root meristem growth and is crucial for root initiation and lateral root number. *AUX1*
450 was translated from *aspen* Potra002054g16021 while *IAA3/SHY2* and *AXR5* were translated from
451 *aspen* Potra000605g04596. For both these aspen genes, generated aspen RNAi lines exhibited an
452 increase in stem diameter, an important indicator for tree biomass yield, connecting back to the
453 underlying regulatory processes in the meristematic tissues (Table S2). *AUX1* is an auxin
454 transport protein which regulates auxin distribution across source (young leaf) and sink organs
455 (young roots) (Marchant et al., 2002). *IAA3/SHY2* is crucial for root meristem development in
456 Arabidopsis, being the converging point of cytokinin and auxin regulatory circuit (Li et al.,
457 2020). Arabidopsis mutants for *AUX1* and *IAA3/SHY2* showed alterations in number and size of
458 lateral roots (Tian and Reed, 1999; Marchant et al., 2002) while *AXR5* is an auxin response
459 factor and mutant plants for this gene are resistant to auxin and show alterations of root and
460 shoot tropisms (Yang et al., 2004). Our network results and phenotypes in aspen and Arabidopsis
461 indicate that these genes also play an import role in meristem growth in other organs apart from
462 root. *HBII*, *AIF3*, and *AIF4*, encode a tier of interacting bHLH transcription factors downstream
463 of BR and regulate the cell elongation in leaf blade and petiole (Bai et al., 2013; Ikeda et al.,
464 2013). *AIF3* and *AIF4* were translated from Potra004144g24626 while *HBII* was translated from
465 Potra186144g28414. These two aspen genes have been tested with an overexpression approach

466 in aspen trees showing even a bigger increase in stem diameter as compared with the auxin-
467 related aspen genes Potra000605g04596 and Potra002054g16021 (Table S2). Arabidopsis
468 mutants for these genes (*HBII*, *AIF3*, and *AIF4*) have been linked with alteration of petiole
469 length (Table S7).

470 *LMI2* was a highly ranked IYG prediction. Importantly, *LMI2* (a MYB TF) is not a paralog of
471 *LATE MERISTEM IDENTITY 1* (*LMII*, a homeobox TF), also predicted here. Although *LMII*
472 and *LMI2* belong to different TF families, they both function downstream of LEAFY to regulate
473 meristem transition (Pastore et al., 2011). *LMII* was reported to regulate leaf growth in
474 Arabidopsis and other species (Vlad et al., 2014; Andres et al., 2017; Li et al., 2021).
475 Arabidopsis *LMII* loss-of-function mutant showed decreased leaf serration and promoted tissue
476 growth in stipules (Vuolo et al., 2018). The observed phenotype of mutated *LMI2* was related to
477 an increase of the number of cauline leaves and secondary inflorescences (Pastore et al., 2011).
478 Here, *LMI2* transgenic lines were subjected to phenotypic analysis, which demonstrated that a
479 *LMI2* loss-of-function mutant showed increased rosette area. The neighbourhood conservation of
480 both *LMII* and *LMI2* suggests that it would be worthwhile to further explore their roles in leaf
481 shape control across monocots and dicots.

482 Other known examples of functionally conserved predictions across monocots and dicots were
483 GRFs (e.g. the highly ranked *GRF2*), which have a recognized role in leaf size regulation, and
484 AN3/GIF1, a transcriptional co-activator protein (Nelissen et al., 2016). This was also testified
485 by their network conservation in stringent density subnetworks (DS2). A second gene *GLI*, had
486 its network neighbourhood conserved with GRMZM2G022686 from maize. This maize gene
487 encodes for the MYB-related protein *Myb4*. This protein plays important roles in plant improved
488 tolerance to cold and freezing in Arabidopsis and barley (Soltész et al., 2012), but no connections
489 with improved yield have been observed for this gene. Arabidopsis *SUC2* showed conservation
490 with GRMZM2G307561, a sucrose/H⁺ symporter which remobilize sucrose out of the vacuole to
491 the growing tissues. Mutants for this gene showed reduced growth and the accumulation of large
492 quantities of sugar and starch in vegetative tissues in Arabidopsis (Srivastava et al., 2008), while
493 in maize mutants, slower growth, smaller tassels and ears, and fewer kernels were observed
494 (Leach et al., 2017). This gene is thus also important for growth, development, and yield across
495 monocots and dicots.

496 A total of 11 primary-IYGs from Arabidopsis showed no network neighbourhood conservation.
497 Lack of conservation might be the result of (1) missing orthologs in a target species or (2)
498 different set of co-expressing genes across species, which in turn might be caused by different
499 transcriptional control. One clear example of no conservation due to a lack of orthologs is
500 PEAPOD 2 (*PPD2*), which is a TIFY transcriptional regulator part of the PEAPOD (PPD)
501 pathway. This pathway plays an important role in cell proliferation and, with its PPD/KIX/SAP
502 module, is involved in leaf, flower, fruit, and seed development. This pathway is highly
503 conserved among flowering plant species but absent in monocot grasses (Schneider et al., 2021).
504 The reason for this absence might be found back in intrinsic differences between eudicots and
505 grasses, being mainly lack of meristemoids and functional redundancy for the regulation of cell
506 proliferation. Surprisingly, several non-grass monocot species such as *Musa acuminata* (banana)
507 and *Elaeis guineensis* (oil palm), basal angiosperm *Amborella trichopoda* and lycophytes, carry
508 PPD/KIX/SAP orthologs, although information about their functionality is missing (Schneider et
509 al., 2021). Another gene with orthologs but lacking network neighborhood conservation was
510 *AHK3*, a cytokinin receptor that controls cytokinin-mediated leaf longevity. This might be
511 explained by knock-out experiments on *AHK* receptors showing contrasting effects on flowering
512 time or floral development across Arabidopsis and rice (Burr et al., 2020). Another non-
513 conserved IYG was *ZHD5* that regulates floral architecture and leaf development and is
514 regulated by *MIF1* (*MINI ZINC-FINGER 1*) (Hong et al., 2011), which also lacked network
515 conservation. *ZHD5* regulation might thus be different across species. Similarly, *FBX92* (*F-BOX*
516 *PROTEIN92*) was not conserved, which might be explained by the opposite effects on leaf size
517 shown by *ZmFBX92* and *AtFBX92* gain of function in Arabidopsis due to the presence of an F-
518 box-associated domain in *AtFBX92*, lacking in *ZmFBX92*. *FBX92* orthologs might thus undergo
519 different transcriptional regulation (Baute et al., 2017). *EPF1* (*EPIDERMAL PATTERNING*
520 *FACTOR 1*) was also a non-conserved IYG. This gene affects stomatal density and water use
521 efficiency. Recent work suggested that, in monocots and dicots, *EPF1* orthologs probably have
522 different temporal dynamics of gene expression in the stomatal lineage (Buckley et al., 2020),
523 which might result in different co-expressors.

524

525 Based on the validation results of our IYG prediction pipeline, a correlation between network
526 size and recovery of genes affecting leaf size was observed. In particular, the most stringent

527 Arabidopsis network showed a high recovery rate of leaf phenotype related genes, either
528 considering RARGE II leaf trait genes or an in-depth literature analysis. With increasing network
529 size, the recovery rate decreased. The network neighborhood conservation of genes in the most
530 stringent networks involved different fundamental processes, suggesting their functional
531 similarity across monocots and dicots. Not surprisingly, genes involved in cell cycle regulation
532 and plant hormonal response were found, as both processes have a key role in leaf development.
533 Several cell cycle regulators were predicted as IYGs, like the cyclin gene *CYCD3;3*, the *CDK*
534 inhibitor *KRP3 (KIP-RELATED PROTEIN)*, and a DOF transcription factor gene *OBP1 (OBF*
535 *BINDING PROTEIN 1)* that controls cell cycle progression (Dewitte et al., 2007; Skirycz et al.,
536 2008; Jun et al., 2013). The auxin-responsive transcription factor gene *MONOPTEROS (MP)* is
537 crucial for leaf vascular development (Hardtke and Berleth, 1998), while the Aux/IAA gene that
538 represses auxin signaling, *AXR2*, whose gain-of-function leads to strong inhibition of leaf growth
539 (Mai et al., 2011), was also predicted. Besides auxin, brassinosteroid (BR) and gibberellin (GA)
540 coordinately play key roles in regulating plant cell elongation. The other two predicted
541 transcription factor genes, *HB25 (HOMEODOMAIN PROTEIN 25)* and *MYR1*, which modulate
542 bioactive GA biosynthesis, were also shown to have an effect on the petiole growth (Bueso et al.,
543 2014). It is noteworthy that nearly half of all the 34 genes with leaf phenotype were transcription
544 regulators, which highlights the importance of TF-mediated gene expression regulation during
545 leaf development. In addition to hormone-related genes and TFs, genes related to photosynthesis
546 are also important for leaf development. A carotenoid biosynthesis gene *LCY* and a chloroplast
547 redox-regulating gene *THIOREDOXIN X* were predicted as IYG and have been shown to affect
548 leaf size (Li et al., 2009; Pulido et al., 2010). Moreover, the cytoplasmic carbonic anhydrase
549 genes *CA2* and *BCA4* were identified, consistent with the view that carbon utilization in leaves is
550 closely linked to leaf area (DiMario et al., 2016). Cell wall modification is considered to be
551 another important determinant of leaf development. The predicted candidate genes *LACCASE11*
552 (*LAC11*) and *CUTICLE DESTRUCTING FACTOR 1 (CDEF1)*, encoding for a laccase that
553 associates with the lignin deposition in cell wall and a cutinase essential for the degradation of
554 cell wall components, respectively, are also involved in regulating leaf growth and morphology
555 (Takahashi et al., 2010; Qin et al., 2013). Among Arabidopsis genes with a reported phenotype
556 in the RARGE II loss-of-function dataset, *ACO2 (ACC OXIDASE 2)* led to increased leaf size,
557 and *AT3G43270*, a member of Plant invertase/pectin methylesterase inhibitor superfamily, to

558 smaller leaves. IYGs translated from aspen led, through our integrative network approach, to the
559 prediction of *NITRATE TRANSPORTER 1.3 (NPF6.4/NRT1.3)* as a new potential IYG. In our
560 experiments, we showed that this gene, when mutated, is altering leaf growth. It was previously
561 hypothesized that *NPF6.4/NRT1.3* may play a role in supplying nitrate to photosynthesizing cells
562 (Tong et al., 2016). This cross-species conserved gene would thus contribute to nitrogen
563 assimilation, that, closely interacting with carbon metabolism, sustains plant growth and
564 development (Nunes-Nesi et al., 2010).

565 In conclusion, the approach developed in this study fully exploits the potential of integrative
566 biology to translate and expand yield-related functional annotations in different plant species, as
567 such accelerating crop breeding.

568

569

570 **Methods**

571 **Integration of developmental expression datasets and network construction**

572 Transcriptomic datasets were obtained from a list of studies in Arabidopsis, maize and aspen
573 covering samples from the main leaf developmental phases (Table S1, Supplemental Methods,
574 Dataset 1). Details about processing of these samples were reported in TableS1. Maize data was
575 mainly composed by a developmental compendium newly generated in this work (Supplemental
576 Methods). The network inference was carried out with Seidr (Schiffthaler et al., 2018), which
577 infers gene networks by using multiple inference algorithms and then aggregating them into a
578 meta-network. This approach has been shown to strongly improve the accuracy of the results
579 (Marbach et al., 2012). Each network was subset into five density subnetworks (DSs) using five
580 different network density values. This procedure consisted in selecting the top 0.1, 0.5, 1, 5 and
581 10% top Seidr links in each species-specific network and generating five DSs (from the most
582 stringent DS1 to the least stringent DS5).

583 **Orthology and network neighborhood conservation**

584 In order to compute cross-species gene network neighborhood conservation, orthology
585 information between genes from Arabidopsis, maize and aspen was computed using the PLAZA
586 comparative genomics platform (Van Bel et al., 2018). A custom version of this platform was
587 built covering in total 15 eukaryotic species including *Arabidopsis thaliana* (TAIR10),
588 *Eucalyptus grandis* (v2.0), *Populus trichocarpa* (v3.01), *Populus tremula* (v1.1), *Vitis vinifera*
589 (12X March 2010 release), *Zea mays* (AGPv3.0), *Oryza sativa ssp. Japonica* (MSU RGAP 7),
590 *Triticum aestivum* (TGACv1), *Amborella trichopoda* (Amborella v1.0), *Picea abies* (v1.0),
591 *Pinus taeda* (v1.01), *Selaginella moellendorffii* (v1.0), *Physcomitrella patens* (v3.3),
592 *Chlamydomonas reinhardtii* (v5.5) and *Micromonas commode* (v3.0). PLAZA allows identifying
593 orthologs using different methods (evidences), corresponding to orthologous gene families
594 inferred through sequence-based clustering with OrthoFinder (Emms and Kelly, 2015),
595 phylogenetic trees, and multispecies Best-Hits-and-Inparalogs families (van Bel et al., 2012).
596 The PLAZA orthology relationships were extracted and filtered retaining all orthologs having a
597 requirement of 2/3 orthology evidences and, for those with 1/3 evidence and >25 orthologs, the
598 ones corresponding to the best 25 blast hits (sorted by e-value) were retained. The generated
599 orthology output was used for the following pipeline steps.

600 The generated DSs and the orthology information were used to compare the three species using a
601 network neighborhood conservation analysis (ComPIEx analysis, as in Netotea et al.). In this
602 analysis, the co-expression of a gene was considered conserved if its network neighborhood (i.e.
603 all genes with a link to it) had a statistically significant ($q < 0.05$) overlap with the network
604 neighborhood of its ortholog in the other species (Netotea et al., 2014). Here, the comparison
605 was performed for all pairs of networks between the datasets of the three species, and the output
606 of this analysis was collated to create “triplets”. The triplets are sets of three orthologous genes—
607 one per network/species—that have a significantly conserved network neighborhood in all three
608 pairs of comparisons. Since the test is not commutative, the neighborhoods had to be
609 significantly conserved in both directions of the test. To estimate the false discovery rate (FDR)
610 of the detection of triplets, a permutation strategy was adopted. For 500 runs of ComPIEx,
611 ortholog relationships were shuffled, keeping the relative number of orthologs per gene and per
612 species, and then comparing the number of triplets computed from randomization with those
613 resulting using the original (unshuffled) orthologs.

614 **Functional information for gene function prediction**

615 Gene Ontology (Ashburner et al., 2000) functional annotations for Arabidopsis, maize and aspen
616 were retrieved from TAIR (download 25/12/2018), Gramene (AGPv3.30,
617 <http://bioinfo.cau.edu.cn/agriGO/download.php>) and PlantGenIE
618 (ftp://ftp.plantgenie.org/Data/PopGenIE/Populus_tremula/v1.1/annotation/), respectively, and
619 filtered for the genes present in the corresponding species networks. We focused on biological
620 processes (BP) and excluded the general GO BP terms with ≥ 1500 genes as well as GO terms
621 with ≤ 10 genes to avoid biases towards very general (e.g. biological regulation) and specific
622 terms. For each gene, all GO annotations were recursively propagated in order to include
623 parental GO terms. To get a complete view on all relevant processes related to plant yield,
624 information from literature was collected on intrinsic yield genes (IYGs). Experimentally
625 validated genes in Arabidopsis, maize and aspen (primary-IYGs) were retrieved from public
626 databases (Gonzalez et al., 2010; Beltramino et al., 2018). A second set of experimentally
627 validated aspen genes were obtained by access to SweTree Technologies' private database that
628 contains data from the large-scale testing of $>1,000$ genes and their yield-related properties, an
629 effort where more than 1,500 recombinant DNA constructs were used to either introduce a new
630 gene product or alter the level of an existing gene product by over-expression or RNA

631 interference in aspen trees, whose growth characteristics were then monitored in greenhouse and
632 field experiments to provide extensive gene-to-yield data. The Arabidopsis IYG primary set was
633 then enlarged with high quality IYG orthologs from maize and aspen using the triplets
634 (“translated-IYGs”) to obtain a combined IYG set. The combined set was finally filtered with
635 genefilter package for Bioconductor (Gentleman et al., 2021) to remove genes with small
636 expression variance ($\text{var.func}=\text{IQR}$, $\text{var.cutoff}=0.8$) and focus on genes active during
637 proliferation or expansion phases of leaf development (“expression-supported IYGs”, Table S2).
638 Other information on functional categories (Vercruyssen et al., 2020) (Table S3) and differentially
639 expressed genes from relevant studies on plant development was also included in the functional
640 enrichment analyses (Anastasiou et al., 2007; Gonzalez et al., 2010; Eloy et al., 2012;
641 Vercruyssen et al., 2014).

642 The expression-supported IYG set was used to perform network-guided gene function prediction
643 via a guilt-by-association (GBA) approach. This approach is based on the assumption that genes
644 close to the input IYGs in the network are likely to have similar functions. The GBA approach
645 was applied to attribute new functions based on GO enrichment in the modules of each DS
646 yielding five sets of gene predictions. By this procedure, gene neighborhoods significantly
647 enriched for known IYGs were functionally annotated (hypergeometric distribution). This
648 allowed to predict new IYGs and estimate, for each of them, a corresponding FDR adjusted p-
649 value (or q-value), which was renamed “GBA-score”. The GBA-score is a confidence score that
650 ranks genes low if they are connected with many IYGs in the network being a low score and
651 indicator of strong enrichment. For an example IYG prediction (in one of any of the five DSs),
652 the GBA-score from the five DSs was summarized taking the mean of the GBA-scores and
653 setting the GBA-score to 0.05 for the DSs where the gene was not predicted. This yielded a list
654 of IYG predictions that was then further filtered by only retaining those predictions having
655 conserved neighborhood in at least one DS.

656 **Validation of IYG predictions using large-scale phenotyping data**

657 To perform a validation of the gene function predictions, the RARGE II (Akiyama et al., 2014)
658 database was interrogated to retrieve a list of Arabidopsis genes that, when mutated, showed an
659 increased or decreased length, width and size for rosette leaf, vascular leaf and cauline leaf (leaf
660 trait genes). The IYG prediction list was split according to the DS conservation of the predictions

661 in five subsets. Each subset was analyzed for over-representation of specific biological process
662 annotations using a functional enrichment analysis, using the hypergeometric distribution
663 together with Benjamini-Hochberg (BH) correction for multiple testing (Benjamini and
664 Hochberg, 1995). A similar approach was used to explore the top 100 predictions ranked by
665 GBA-score. In this case a manual literature search was performed to retrieve all genes with a
666 reported phenotype including information about the biological pathway the gene might be active
667 in, and other public functional annotations.

668 **Rosette growth phenotyping**

669 The *Arabidopsis thaliana* ecotype Columbia-0 (Col-0) was used as the wild-type in this study.
670 The T-DNA insertion lines for At4g26530 (Salk_080758/*fba5-1*), At3g21670
671 (Salk_001553/*sper3-3*), At3g61250 (Salk_066767/*lmi2-1*, Salk_020792/*lmi2-2*), At4g25240
672 (Salk_113731), At1g63470 (Salk_123590/*ahl5*), At4g37980 (Salk_001773/*chr hpl*), At2g38530
673 (Salk_026257/*ltp2-1*), At4g28950 (Salk_019272), and At1g12240 (Salk_016136) were
674 confirmed using PCR with a T-DNA primer and gene-specific primers (Lu et al., 2012; Zhao et
675 al., 2013; Jacq et al., 2017; Tanaka et al., 2018; Pastore et al., 2011; Tong et al., 2016). All tested
676 seeds were stratified in the darkness at 4 °C for 3 days and then sown on soil in the 7 cm wide
677 square pots with a density of four seeds per pot. After 8 days in the growth room (with controlled
678 temperature at 22 °C and light intensity 110 $\mu\text{mol m}^{-2} \text{s}^{-1}$ in a 16 h/8 h cycle), the four seedlings
679 were screened, leaving one seedling per pot, which most closely resembled the genotype
680 average. The plants were imaged in a phenotyping platform (MIRGIS) with fixed cameras
681 located directly above the plants, which images plants at the same time every day. These images
682 were then processed to extract the rosette growth parameters of each plant. The mean PRA,
683 compactness and stockiness values were calculated over time for each genotype.

684 **Author Contributions**

685 P.L.C, N.S, T.R.H, H.N and K.V designed the research; P.L.C, J.Z, N.M, C.S, C.M, T.D, and
686 T.V.H performed research and data analysis; N.M, T.V.H, D.J, and M.H contributed new data
687 and analytic tools, P.L.C, J.Z and K.V wrote the paper with input from all co-authors.

688 **Accession Numbers**

689 Sequence data from this article have been submitted to ENA (E-MTAB-11108).

690 **Supplemental data**

691 Supplemental Figure 1. Number of neighbors per gene at each density subnetwork in
692 Arabidopsis.

693 Supplemental Figure 2. Expression patterns for the expression-supported intrinsic yield gene set
694 in Arabidopsis.

695 Supplemental Figure 3. Expression supported IYGs with neighborhood conservation at each
696 density level.

697 Supplemental Figure 4. Functional enrichment of cross-species conserved transcription factors
698 (TF) grouped by TF family.

699 Supplemental Figure 5. Identification of T-DNA insertion lines.

700 Supplemental Table 1. Overview of the expression datasets used for the network computation

701 Supplemental Table 2. List of expression-supported intrinsic yield genes

702 Supplemental Table 3. Yield functional categories and genes in Arabidopsis

703 Supplemental Table 4. Intrinsic yield gene predictions

704 Supplemental Table 5. List of RARGE II leaf trait genes known to affect leaf phenotype if
705 mutated

706 Supplemental Table 6. Top 100 intrinsic yield gene predictions annotated

707 Supplemental Table 7. In depth literature analysis for the top 100 intrinsic yield gene predictions

708 Supplemental Table 8. List of genes tested for leaf phenotype in this study

709 Supplemental Dataset 1. Expression datasets for Arabidopsis, maize, and aspen

710 Supplemental Data set 2. Triplets generated with ComPIEx

711 Supplemental Methods. Detailed methods for expression dataset retrieval, generation, and
712 processing.

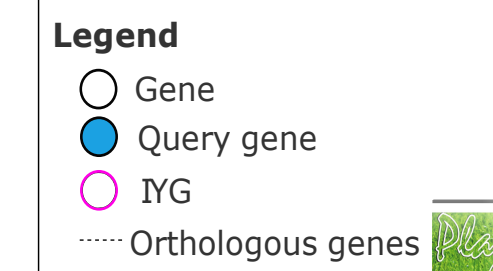
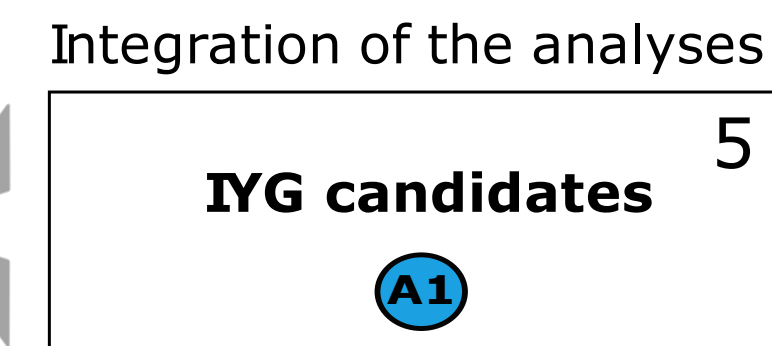
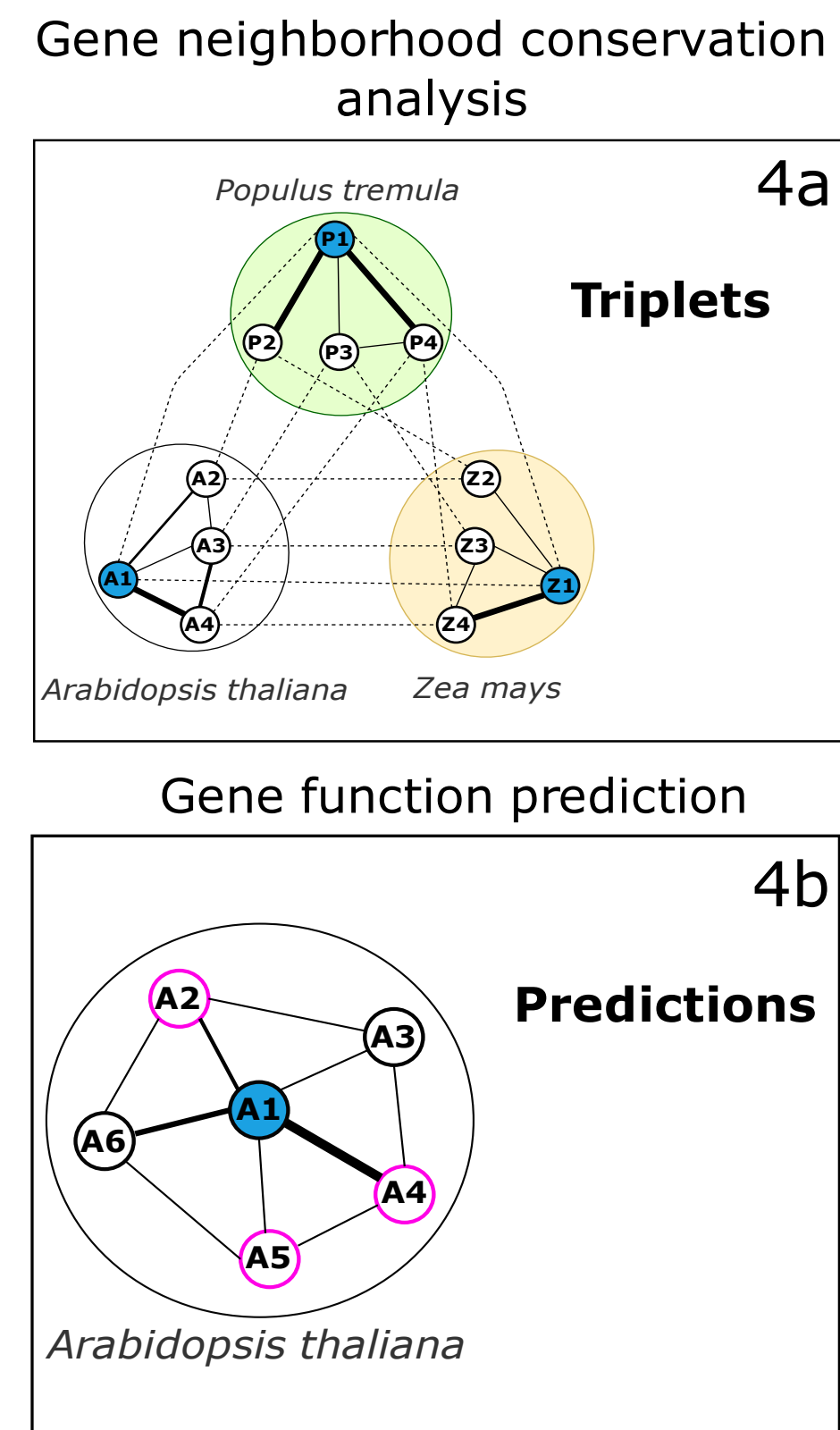
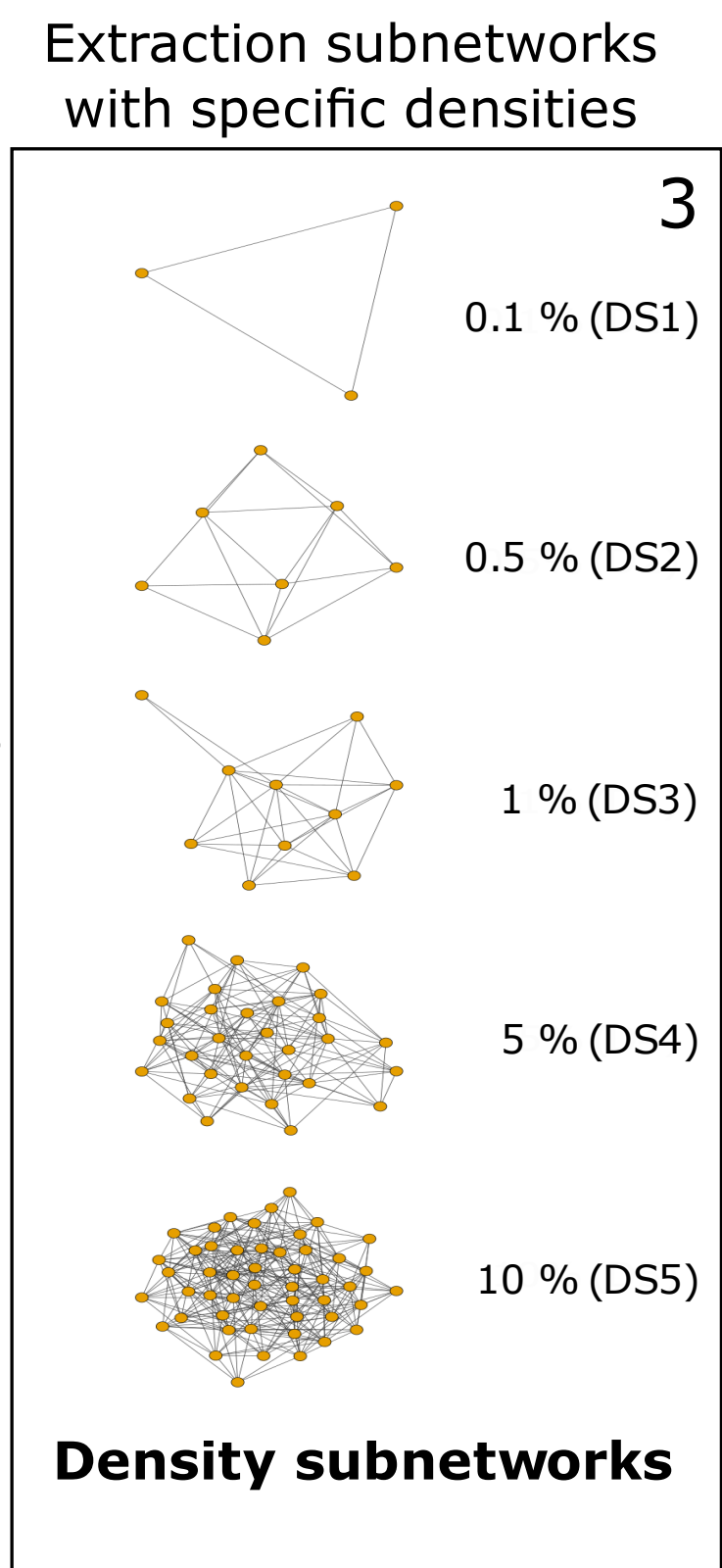
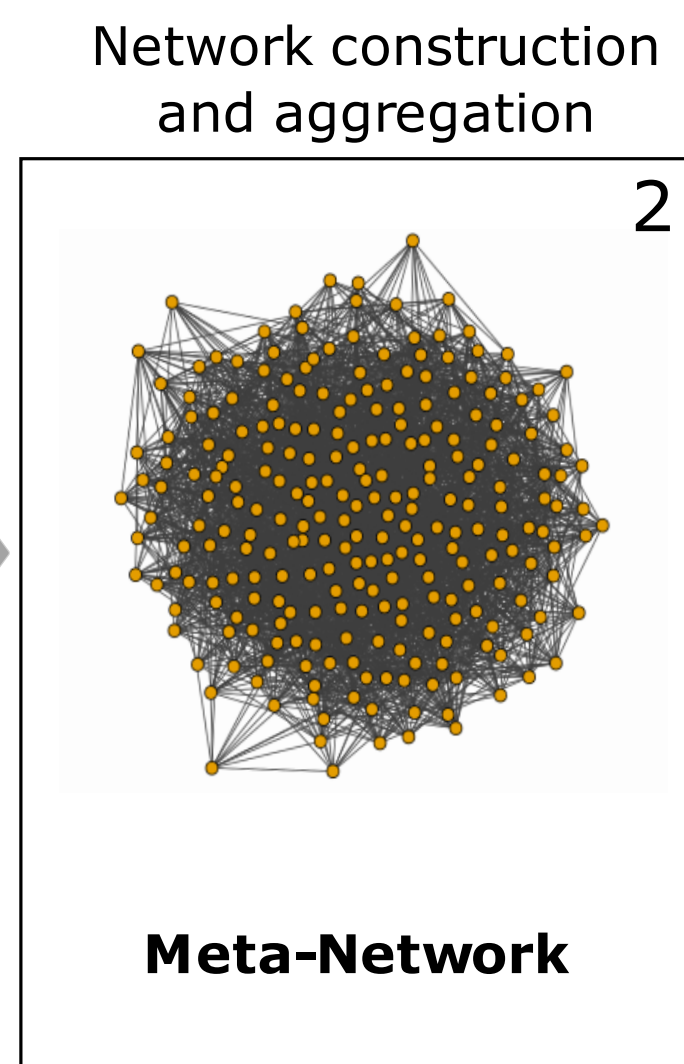
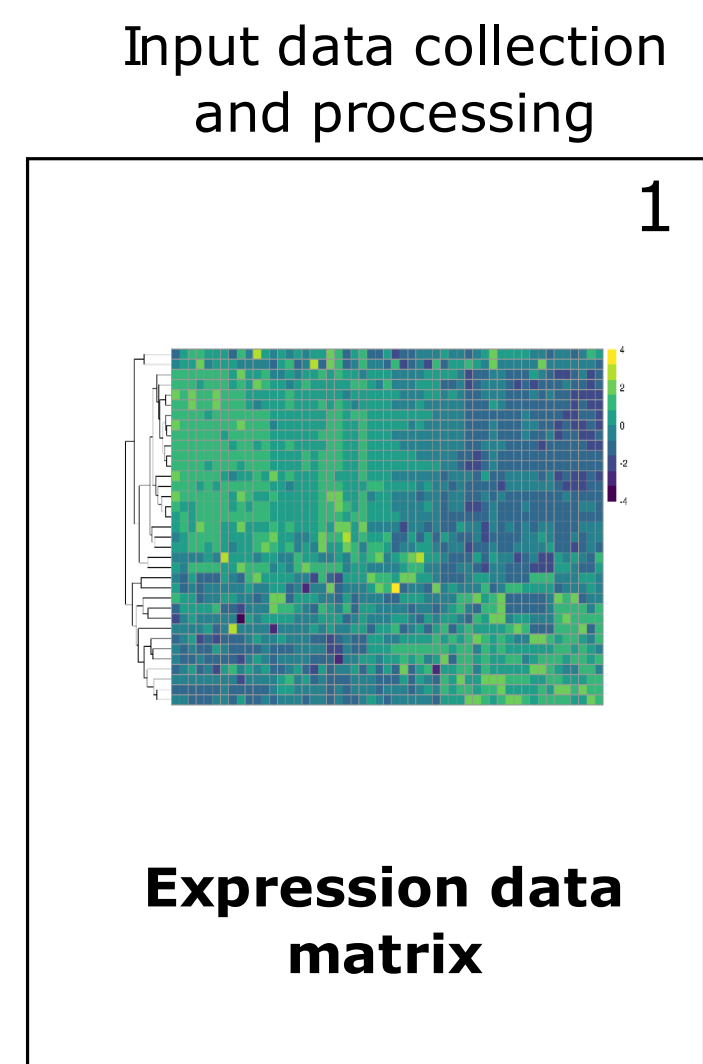
713 **Acknowledgements**

714 We thank Julie Pevernagie for her technical support.

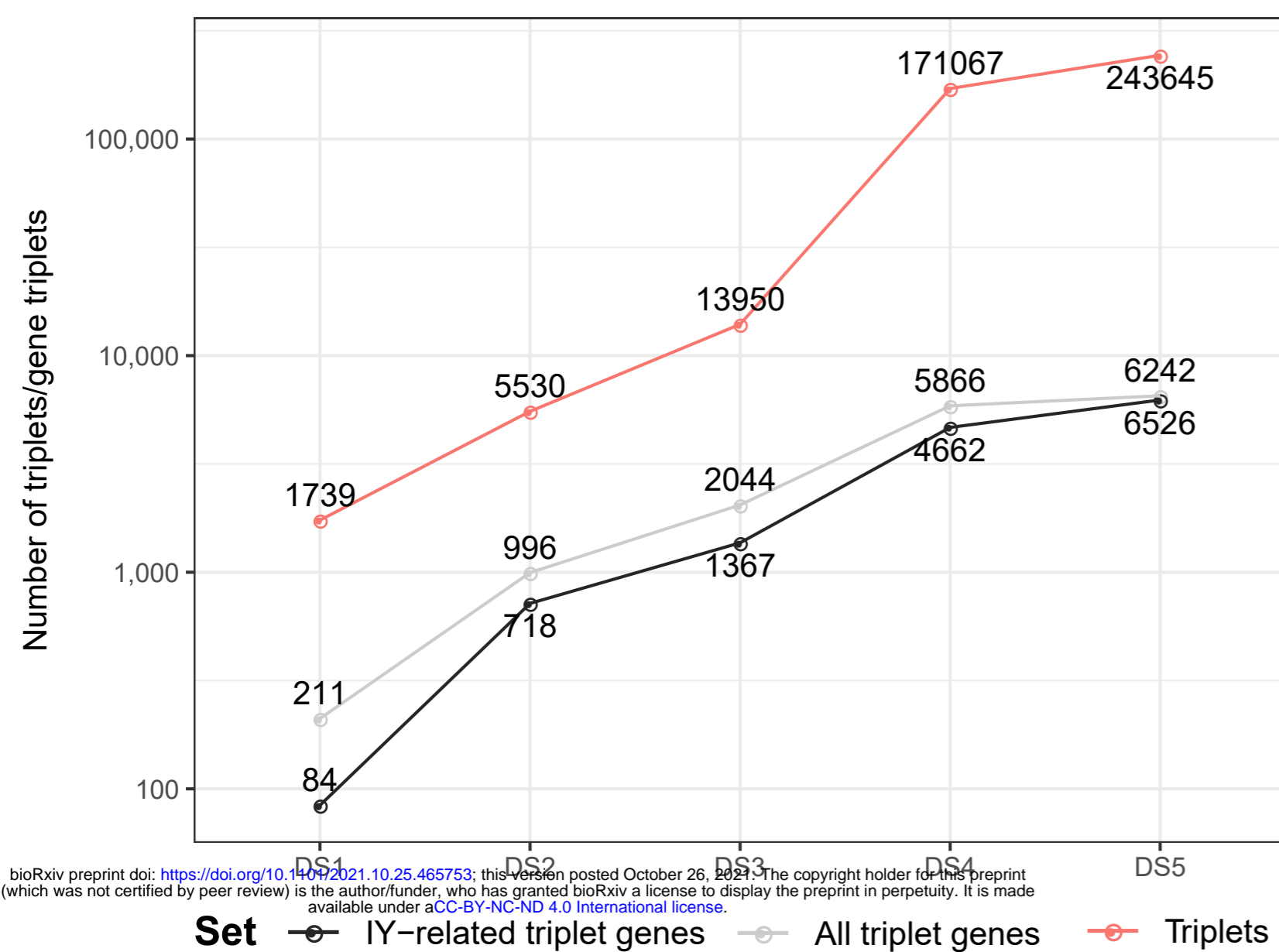
715 **Funding**

716 **TRH, KV and NRS was partially funded by the Research Council of Norway (project**
717 **number 287465).**

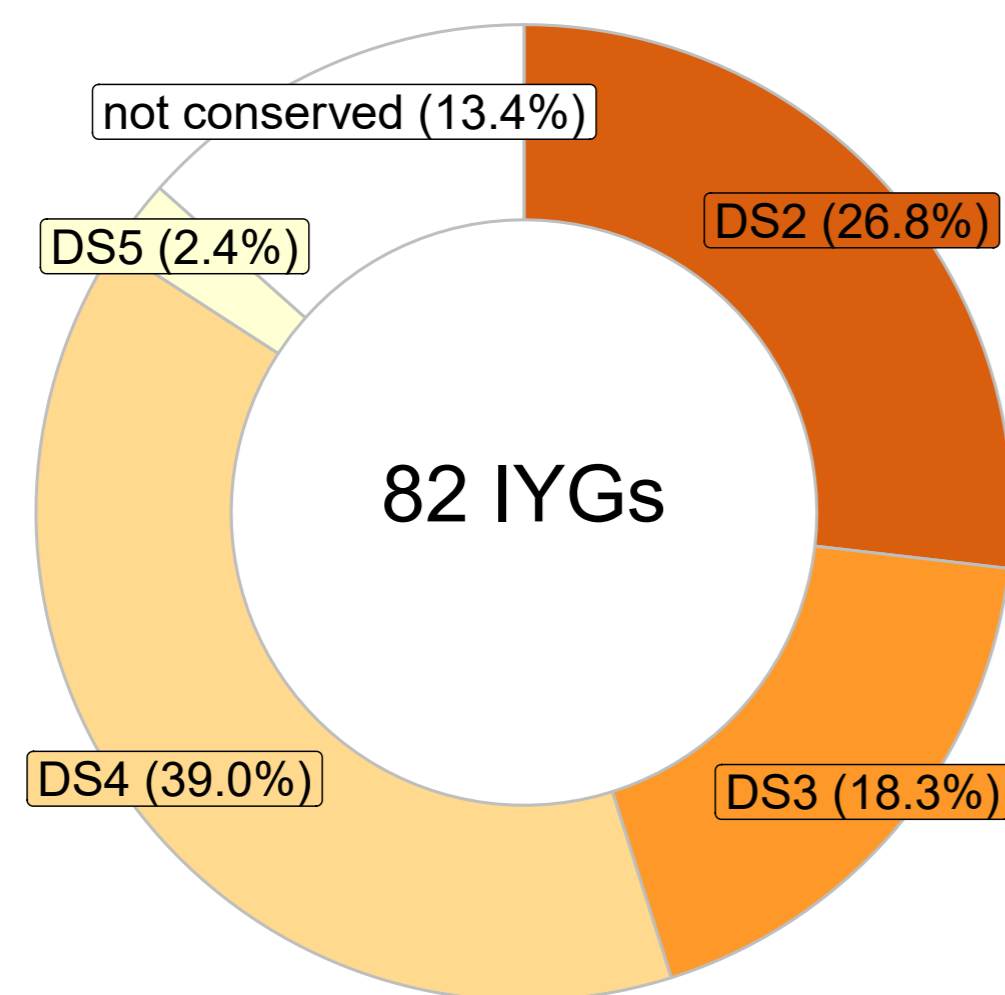
718



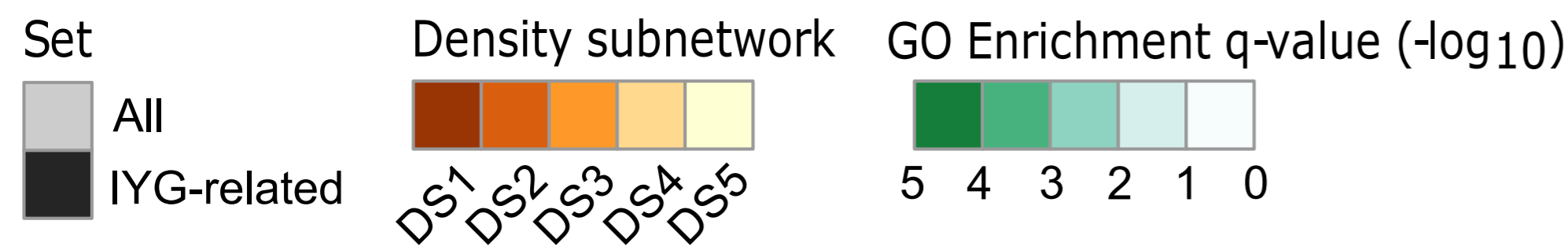
A



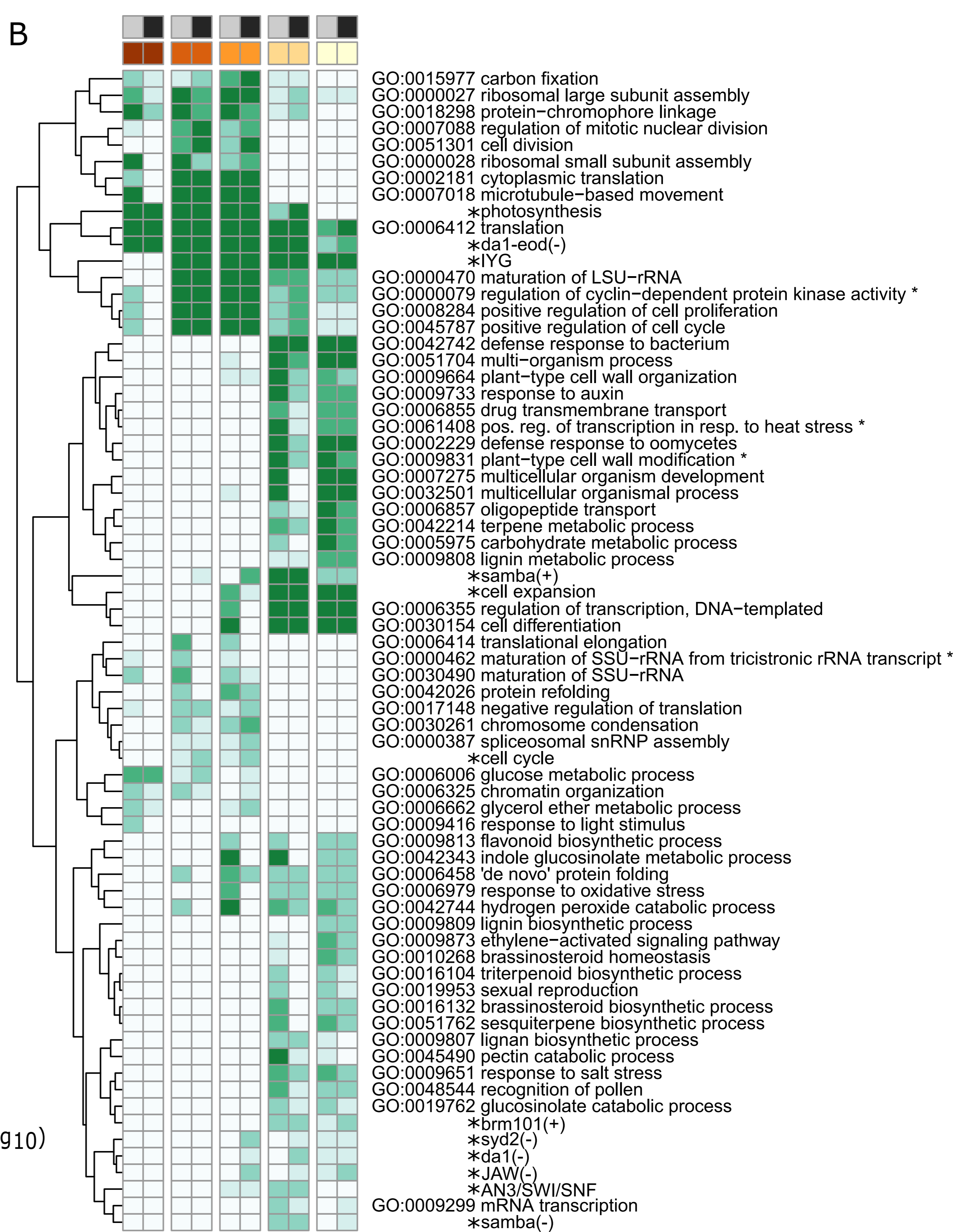
C



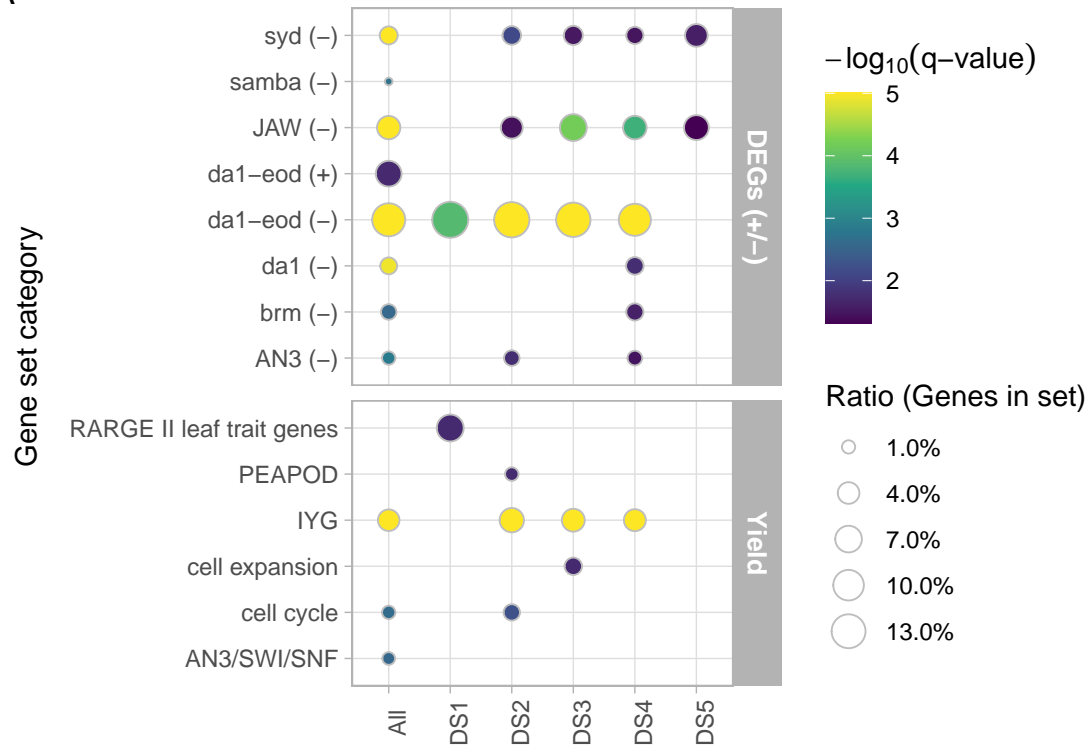
Legend



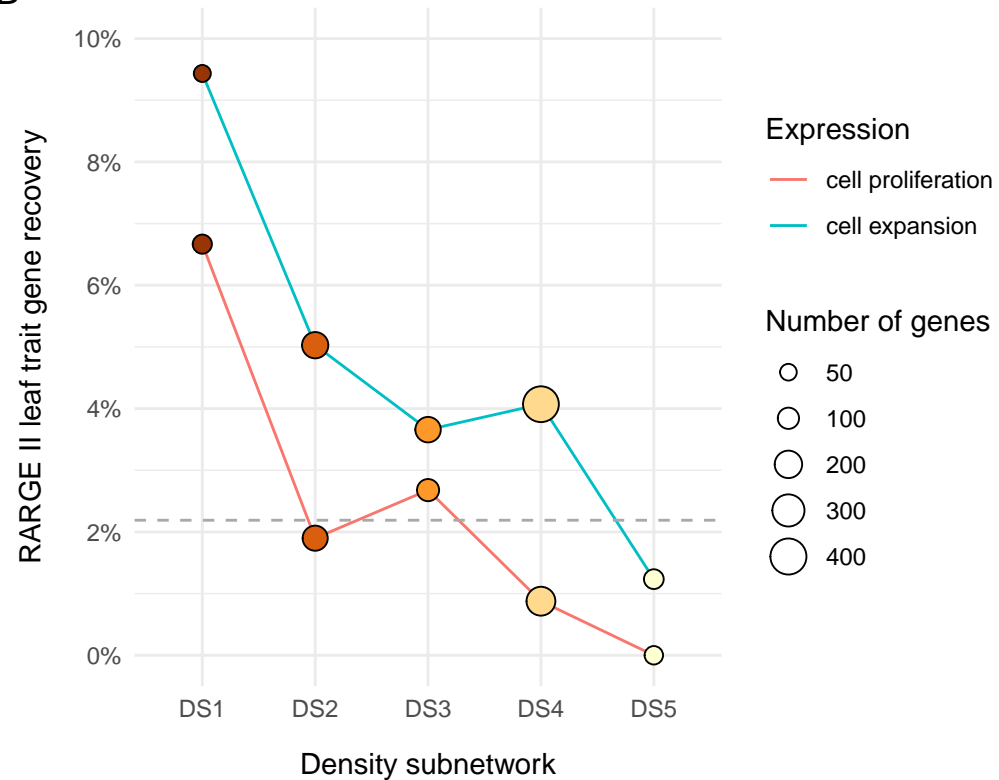
B

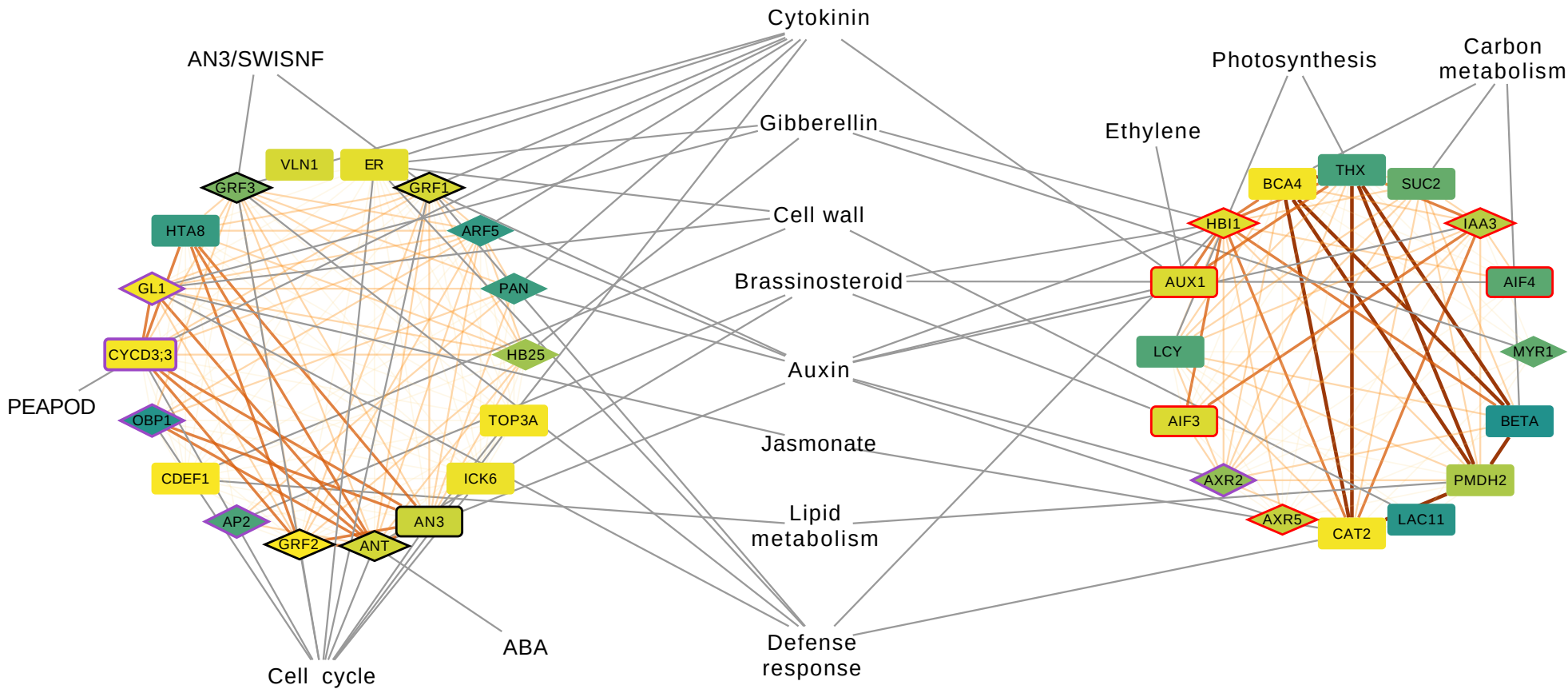


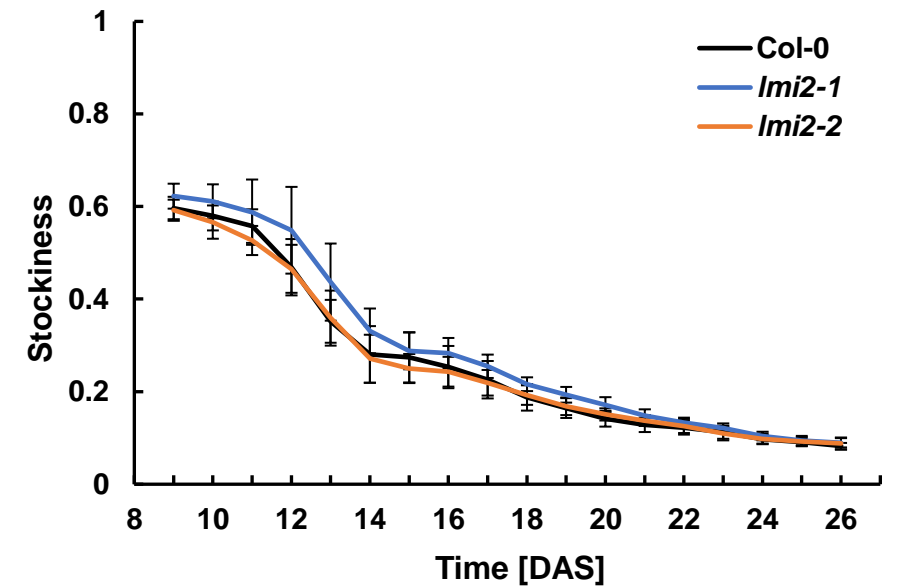
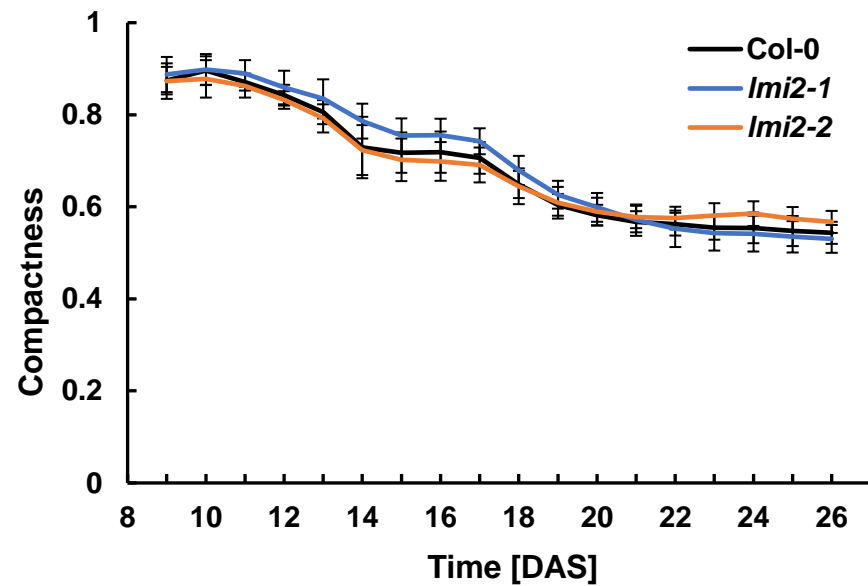
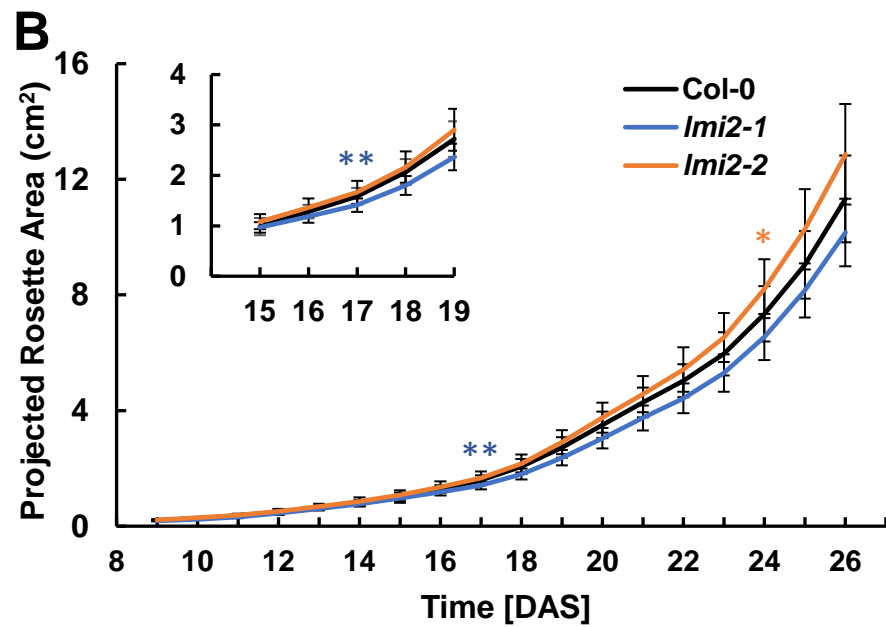
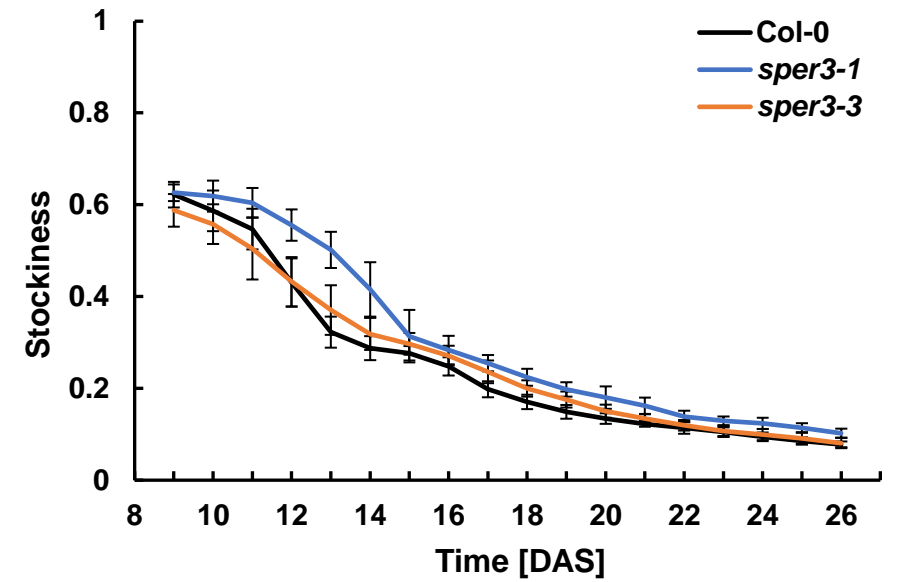
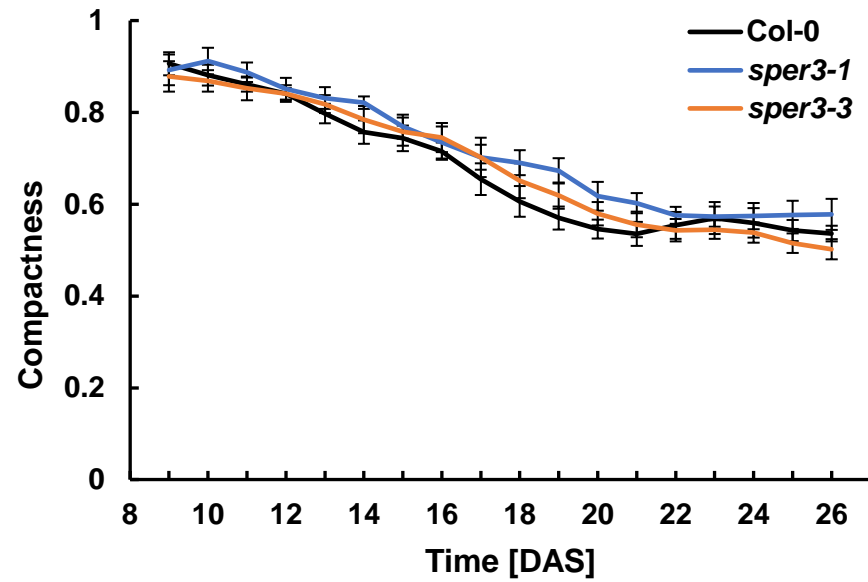
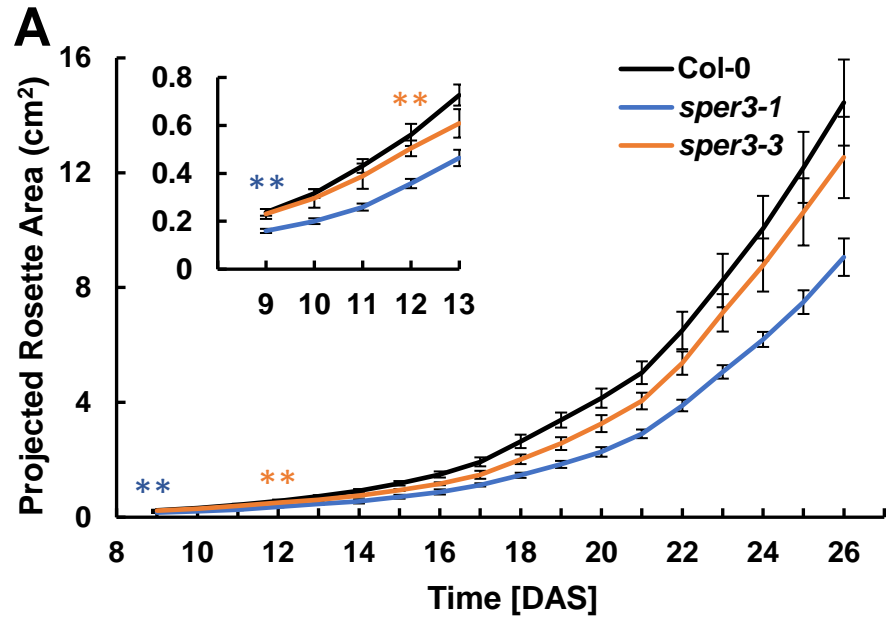
A



B







Parsed Citations

Andriankaja, M., Dhondt, S., De Bodt, S., Vanhaeren, H., Coppens, F., De Milde, L., Mühlhenn, P., Skiryicz, A., Gonzalez, N., Beemster, G.T., and Inzé, D. (2012). Exit from Proliferation during Leaf Development in *Arabidopsis thaliana*: A Not-So-Gradual Process.

Bray, N.L., Pimentel, H., Melsted, P., and Pachter, L. (2016). Near-optimal probabilistic RNA-seq quantification. *Nat. Biotechnol.* 34: 525–527.

Google Scholar: [Author Only Title Only Author and Title](#)

Chotewutmontri, P. and Barkan, A. (2016). Dynamics of Chloroplast Translation during Chloroplast Differentiation in Maize. *PLoS Genet.* 12: 1–28.

Google Scholar: [Author Only Title Only Author and Title](#)

Dubois, M., Claeys, H., Van den Broeck, L., and Inzé, D. (2017). Time of day determines *Arabidopsis* transcriptome and growth dynamics under mild drought. *Plant Cell Environ.* 40: 180–189.

Google Scholar: [Author Only Title Only Author and Title](#)

Heldt, H.-W. and Piechulla, B. (2021) Photosynthesis needs the consumption of water. *Plant Biochemistry (Fifth edition)*: 191-216

Google Scholar: [Author Only Title Only Author and Title](#)

Leek, J.T., Scharpf, R.B., Bravo, H.C., Simcha, D., Langmead, B., Johnson, W.E., Geman, D., Baggerly, K., and Irizarry, R.A. (2010). Tackling the widespread and critical impact of batch effects in high-throughput data. *Nat. Rev. Genet.* 11: 733–739.

Google Scholar: [Author Only Title Only Author and Title](#)

Mähler, N., Schiffthaler, B., Robinson, K.M., Terebieniec, B.K., Vučak, M., Mannapperuma, C., Bailey, M.E.S., Jansson, S., Hvidsten, T.R., and Street, N.R. (2020). Leaf shape in *Populus tremula* is a complex, omnigenic trait. *Ecol. Evol.* 10: 11922–11940.

Google Scholar: [Author Only Title Only Author and Title](#)

Nelissen, H. et al. (2018). The reduction in maize leaf growth under mild drought affects the transition between cell division and cell expansion and cannot be restored by elevated gibberellic acid levels. *Plant Biotechnol. J.* 16: 615–627.

Google Scholar: [Author Only Title Only Author and Title](#)

Schlüter, U. and Weber, A. (2019). Regulation and Evolution of C4 Photosynthesis. *FASEB J.* 33: 183–215.

Google Scholar: [Author Only Title Only Author and Title](#)

Schmittgen, T.D. and Livak, K.J. (2008). Analyzing real-time PCR data by the comparative CT method. *Nat. Protoc.* 3: 1101–1108.

Google Scholar: [Author Only Title Only Author and Title](#)

Skiryicz, A., De Bodt, S., Obata, T., De Clercq, I., Claeys, H., De Rycke, R., Andriankaja, M., Van Aken, O., Van Breusegem, F., Fernie, A.R., and Inzé, D. (2010). Developmental Stage Specificity and the Role of Mitochondrial Metabolism in the Response of *Arabidopsis* Leaves to Prolonged Mild Osmotic Stress. *Plant Physiol.* 152: 226–244.

Google Scholar: [Author Only Title Only Author and Title](#)

Skiryicz, A., Claeys, H., De Bodt, S., Oikawa, A., Shinoda, S., Andriankaja, M., Maleux, K., Eloy, N.B., Coppens, F., Yoo, S.-D., Saito, K., and Inzé, D. (2011). Pause-and-Stop: The Effects of Osmotic Stress on Cell Proliferation during Early Leaf Development in *Arabidopsis* and a Role for Ethylene Signaling in Cell Cycle Arrest. *Plant Cell* 23: 1876–1888.

Google Scholar: [Author Only Title Only Author and Title](#)

Sun, X. et al. (2017). Altered expression of maize PLASTOCHRON1 enhances biomass and seed yield by extending cell division duration. *Nat. Commun.* 8: 14752.

Google Scholar: [Author Only Title Only Author and Title](#)

Thompson, J.A., Tan, J., and Greene, C.S. (2016). Cross-platform normalization of microarray and RNA-seq data for machine learning applications. *PeerJ* 4: e1621.

Google Scholar: [Author Only Title Only Author and Title](#)

Vanechoutte, D. and Vandepoele, K. (2019). Curse: Building expression atlases and co-expression networks from public RNA-Seq data. *Bioinformatics* 35: 2880–2881.

Google Scholar: [Author Only Title Only Author and Title](#)

Wang, Y., Long, S.P., and Zhu, X.G. (2014). Elements required for an efficient NADP-malic enzyme type C4 photosynthesis. *Plant Physiol.* 164: 2231–2246.

Google Scholar: [Author Only Title Only Author and Title](#)

Andriankaja, M., Dhondt, S., De Bodt, S., Vanhaeren, H., Coppens, F., De Milde, L., Mühlhenn, P., Skiryicz, A., Gonzalez, N., Beemster, G.T., and Inzé, D. (2012). Exit from Proliferation during Leaf Development in *Arabidopsis thaliana*: A Not-So-Gradual Process.

Bray, N.L., Pimentel, H., Melsted, P., and Pachter, L. (2016). Near-optimal probabilistic RNA-seq quantification. *Nat. Biotechnol.* 34: 525–527.

Google Scholar: [Author Only Title Only Author and Title](#)

Chotewutmontri, P. and Barkan, A. (2016). Dynamics of Chloroplast Translation during Chloroplast Differentiation in Maize. *PLoS Genet.* 12: 1–28.

Google Scholar: [Author Only](#) [Title Only](#) [Author and Title](#)

Dubois, M., Claeys, H., Van den Broeck, L., and Inzé, D. (2017). Time of day determines Arabidopsis transcriptome and growth dynamics under mild drought. *Plant Cell Environ.* 40: 180–189.

Google Scholar: [Author Only](#) [Title Only](#) [Author and Title](#)

Heldt, H-W. and Piechulla, B. (2021) Photosynthesis needs the consumption of water. *Plant Biochemistry (Fifth edition)*: 191-216

Google Scholar: [Author Only](#) [Title Only](#) [Author and Title](#)

Leek, J.T., Scharpf, R.B., Bravo, H.C., Simcha, D., Langmead, B., Johnson, W.E., Geman, D., Baggerly, K., and Irizarry, R.A. (2010). Tackling the widespread and critical impact of batch effects in high-throughput data. *Nat. Rev. Genet.* 11: 733–739.

Google Scholar: [Author Only](#) [Title Only](#) [Author and Title](#)

Mähler, N., Schifftaler, B., Robinson, K.M., Terebieniec, B.K., Vučak, M., Mannapperuma, C., Bailey, M.E.S., Jansson, S., Hvidsten, T.R., and Street, N.R. (2020). Leaf shape in *Populus tremula* is a complex, omnigenic trait. *Ecol. Evol.* 10: 11922–11940.

Google Scholar: [Author Only](#) [Title Only](#) [Author and Title](#)

Nelissen, H. et al. (2018). The reduction in maize leaf growth under mild drought affects the transition between cell division and cell expansion and cannot be restored by elevated gibberellic acid levels. *Plant Biotechnol. J.* 16: 615–627.

Google Scholar: [Author Only](#) [Title Only](#) [Author and Title](#)

Schlüter, U. and Weber, A. (2019). Regulation and Evolution of C4 Photosynthesis. *FASEB J.* 33: 183–215.

Google Scholar: [Author Only](#) [Title Only](#) [Author and Title](#)

Schmittgen, T.D. and Livak, K.J. (2008). Analyzing real-time PCR data by the comparative CT method. *Nat. Protoc.* 3: 1101–1108.

Google Scholar: [Author Only](#) [Title Only](#) [Author and Title](#)

Skirycz, A., De Bodt, S., Obata, T., De Clercq, I., Claeys, H., De Rycke, R., Andriankaja, M., Van Aken, O., Van Breusegem, F., Fernie, A.R., and Inzé, D. (2010). Developmental Stage Specificity and the Role of Mitochondrial Metabolism in the Response of Arabidopsis Leaves to Prolonged Mild Osmotic Stress. *Plant Physiol.* 152: 226–244.

Google Scholar: [Author Only](#) [Title Only](#) [Author and Title](#)

Skirycz, A., Claeys, H., De Bodt, S., Oikawa, A., Shinoda, S., Andriankaja, M., Maleux, K., Eloy, N.B., Coppens, F., Yoo, S.-D., Saito, K., and Inzé, D. (2011). Pause-and-Stop: The Effects of Osmotic Stress on Cell Proliferation during Early Leaf Development in Arabidopsis and a Role for Ethylene Signaling in Cell Cycle Arrest. *Plant Cell* 23: 1876–1888.

Google Scholar: [Author Only](#) [Title Only](#) [Author and Title](#)

Sun, X. et al. (2017). Altered expression of maize PLASTOCHRON1 enhances biomass and seed yield by extending cell division duration. *Nat. Commun.* 8: 14752.

Google Scholar: [Author Only](#) [Title Only](#) [Author and Title](#)

Thompson, J.A., Tan, J., and Greene, C.S. (2016). Cross-platform normalization of microarray and RNA-seq data for machine learning applications. *PeerJ* 4: e1621.

Google Scholar: [Author Only](#) [Title Only](#) [Author and Title](#)

Vanechoutte, D. and Vandepoele, K. (2019). Curse: Building expression atlases and co-expression networks from public RNA-Seq data. *Bioinformatics* 35: 2880–2881.

Google Scholar: [Author Only](#) [Title Only](#) [Author and Title](#)

Wang, Y., Long, S.P., and Zhu, X.G. (2014). Elements required for an efficient NADP-malic enzyme type C4 photosynthesis. *Plant Physiol.* 164: 2231–2246.

Google Scholar: [Author Only](#) [Title Only](#) [Author and Title](#)